Analysis of Hydrophone Data for the Coastal Studies Institute
NCROEP Project

Prepared by: S. Lockhart

sblockhart.zzero@gmail.com

May 2021

Table of Contents

Revision History

Date	***Author***	***Description***
5/3/2021	S. Lockhart	This version of the document brings together previous results on this project, which were scattered among several conference presentations (from 2016 to 2019). It also presents the following new or changed material (from 2021): • Updated review of the literature • Click detection using PAMGuard, followed by a machine learning approach to separate clicks from noise, accomplished for all four deployments (three CSI deployments as well as one ADEON deployment) • Whistle detection extended to include the latest CSI deployment. • Fin whale calls detected for all four deployments (three CSI deployments as well as one ADEON deployment)

Coming soon…	S. Lockhart	This version of the document will add the following:
		
		• Baleen whale calls detected for all four deployments (three CSI deployments as well as one ADEON deployment) for the following species:
		  ○ Humpback whales
		  ○ North Atlantic right whales

Introduction

The North Carolina Renewable Ocean Energy Program (NCROEP) has been exploring the prospect of sustainably harnessing Gulf Stream energy off the coast of Cape Hatteras, North Carolina, USA. Characterizing the soundscape in this region is one of the environmental and ecological assessment goals of the program.

This study includes data acquired at the NCROEP mooring site (35°6’ N, 75°5’ W) over three different deployments, totaling about 20 months of data over a period of almost five years (January 2015 to November 2019). It also includes an additional 7 months of data acquired by the Atlantic Deepwater Ecosystem Observatory Network (ADEON), from a mooring approximately 13 km to the northeast of the NCROEP site.

After reviewing the relevant literature, I present the results of a soundscape characterization, including the following:

- Statistics of the long-term average spectra (LTAS) of the underwater sound
- Temporal patterns of several types of marine mammal vocalizations
- Relationship between marine mammal vocalizations and oceanographic variables
- Acoustic propagation models

For marine mammal vocalizations, I detected and analyzed the following sounds:

- Baleen whale sounds, including those produced by fin whales, humpback whales, and North Atlantic right whales
- Toothed whale sounds including clicks, whistles, and dolphin quacks

The complex and dynamic physical oceanography in this region influences the biology as well as the acoustics. Therefore, I combined hydrophone data with oceanographic data and acoustic propagation models, looking for a relationship between marine mammal vocalizations and environmental variables.

Hopefully, this analysis will provide some insight into the acoustic ecology of the region.

Background

Physical oceanography near Cape Hatteras

With variability due the Gulf Stream, the Hatteras Front, air-sea interactions, and other processes, the physical oceanography in this region is complex. These physical processes influence the biology in the ocean as well as the acoustics.

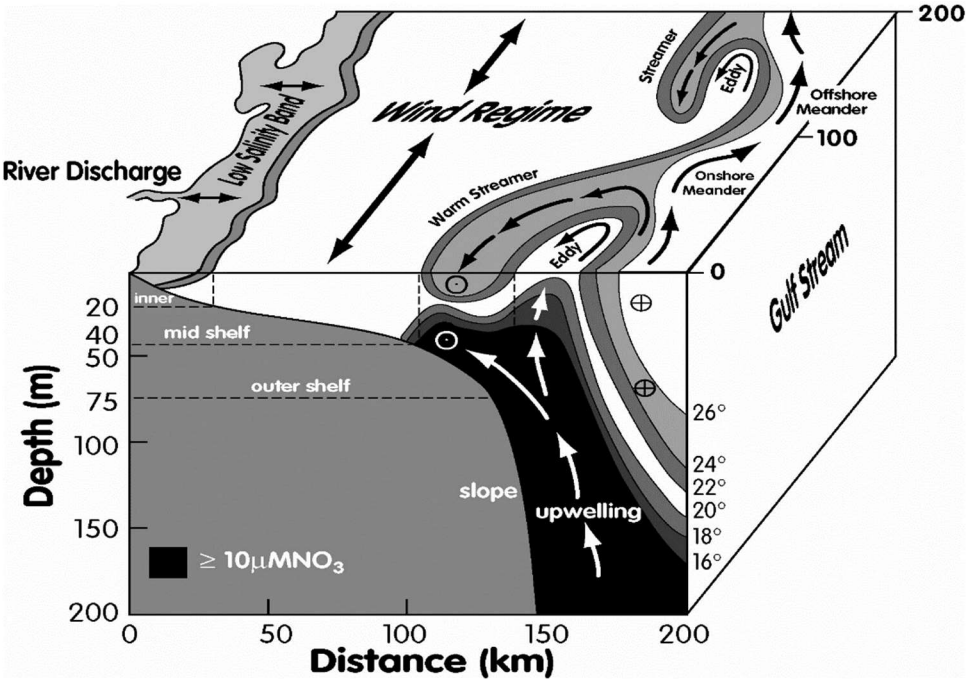

Figure 1: Three-dimensional depiction of Gulf Stream, showing upwelling of cooler, nutrient-rich water into the meander trough, from Jahnke and Blanton (2010)

First, there is variability due to the Gulf Stream, as it meanders back and forth. When the Gulf Stream meanders *offshore*, there may be upwelling of cooler, nutrient-rich water into the meander trough (Jahnke and Blanton, 2010; Hitchcock, 1993; Martins and Pelegri, 1996; Osgood et al., 1987), as illustrated in Figure 1 (from Jahnke and Blanton, 2010).

When the Gulf Stream meanders *onshore*, some meander crests may spawn warm "filaments" (Glenn et al., 1994), labeled "warm streamers" in Figure 1 (from Jahnke and Blanton, 2010).

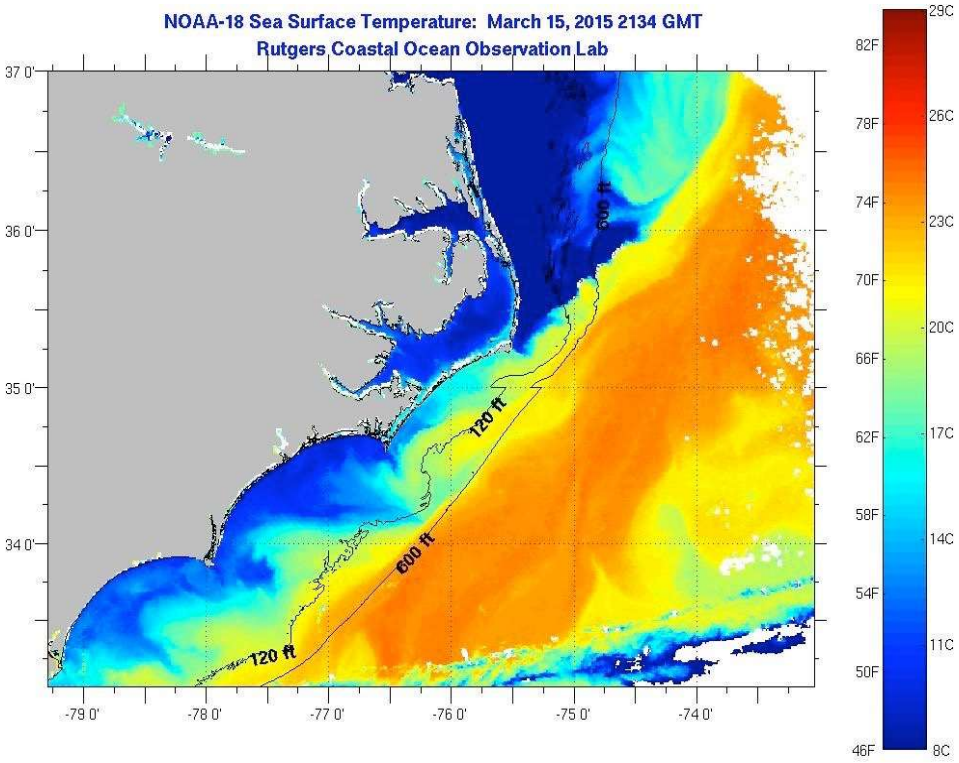

Figure 2: A Sea Surface Temperature (SST) image taken on March 15, 2015 from Rutgers Coastal Ocean Observation Lab, using the Advanced Very High Resolution Radiometer (at https://marine.rutgers.edu/cool/sat_data/?product=sst&region=capehat&nothumbs=0).

In addition to the Gulf Stream Front, there is also the Hatteras Front (Savidge and Austin, 2007), where water from the South Atlantic Bight (SAB) converges with cooler, fresher water from the Mid Atlantic Bight (MAB). In Figure 2, the strong gradient of sea surface temperature (SST) at the Hatteras Front extends northeast from Cape Hatteras.

There can be mixing between these different water masses. For example, there may be *entrainment* of slope water into the Gulf Stream (D'Amico, 1980), or, conversely, *detrainment* of Gulf Stream water onto the slope.

Air-sea interactions are also important in this region. For example, cold air outbreaks in the winter months result in intense exchanges of heat, moisture, and momentum. These events may lead to density-driven cascading or "slumping" of continental shelf water down the continental slope (Shapiro et al., 2003).

Evidence of enhanced productivity at frontal boundaries

Physical processes along fronts often create an environment favorable to marine life (Olson et al., 1994). For example, sampling 154 fronts across the Southern California Current, Powell and Ohman (2015) found increased zooplankton on the denser side of the fronts. This enhanced productivity attracts top predators like marine mammals (Bost et al., 2009; Woodworth et al., 2012; Gilles et al., 2013).

Evidence of marine mammal abundance near Cape Hatteras

Off Cape Hatteras, there is ample evidence that this region is a "hot spot" for many species of marine mammals. In this section, I include the following examples:

- Davis et al. (2020) document one of the most comprehensive surveys of baleen whales in the western North Atlantic. Their analysis combines passive acoustic monitoring data from over 100 research projects, spanning more than 10 years (2004-2014), from the Caribbean to Greenland. One of the regions studied includes Cape Hatteras. For the most part, these baleen whales migrate in and out of the waters around Cape Hatteras, spending summer months at high latitudes and winter months at low latitudes. However, the authors discovered an interesting trend in the distribution of North Atlantic right whales (NARWs): "From 2010 onward, NARWs spent less time in the Gulf of Maine and Bay of Fundy, and more time in mid-Atlantic waters along the US east coast and the Gulf of St. Lawrence", including the Cape Hatteras region. This shift in the distribution of NARW appears to be related to climate change.

- Stanistreet et al. (2018) used passive acoustic monitoring to detect sperm whales at several sites along the east coast of the United States, including a mooring off Cape Hatteras at 35.34N, 74.85W at a depth over 900 meters. This site is about 34 km northeast of the NCROEP mooring. Over a period of almost three years (2013-2015), they found sperm whale activity year-round, with peaks in the winter months.

- Thorne at al. (2017) conclude that "the Cape Hatteras region is an important hotspot of short-finned pilot whale density and foraging habitat."

- Baird et al. (2015) observed and tracked Cuvier's beaked whales, short-finned pilot whales, bottlenose dolphins, and short-beaked common dolphins off the coast of North Carolina, with many sightings on the shelf and slope near the NCROEP mooring site.

- Byrd et al. (2014) looked at data for marine mammal strandings on the beaches of North Carolina. They found a total of 34 different species of marine mammals in 12 years of stranding data.

- A known population of bottle-nosed dolphins in the region of study are usually found south of Cape Hatteras in the winter but north of the cape in the summer (Schick et al., 2011).

- From NOAA NMFS CRUISE RESULTS: NOAA Ship Gordon Gunter Cruise GU-06-03 (2006):

  "During the summer of 2004, a large vessel survey conducted by the SEFSC included concentrated effort in the shelfbreak region of the mid-Atlantic bight ranging from south of

Cape Hatteras, North Carolina to New Jersey. There were very high densities of pilot whales (*Globicephala spp*.), bottlenose dolphins (*Tursiops truncatus*), common dolphins (*Delphinus delphis*), sperm whales (*Physeter macrocephalus*) and other species in the region just north of Cape Hatteras and along the shelf break. The high density and diversity of marine mammals observed is likely associated with the hydrographic complexity in these areas."

Programs monitoring marine mammals near Cape Hatteras

The following table provides links to other programs that monitor marine mammals near Cape Hatteras.

Program	***Dates***	***Description***
Navy Marine Species Monitoring program, Atlantic Fleet Training and Testing (AFTT)	2009 – present	The US Navy monitors marine mammals and sea turtles in order to reduce the impact of naval exercises upon these animals. This program is a collaboration with Duke University, Cascadia Research Collective, Southall Environmental Associates, Sea Mammal Research Unit of the University of St.Andrews, and others. One of the areas studied is the "Cape Hatteras Study Area". Reports are posted at: https://www.navymarinespeciesmonitoring.us/reporting/atlantic/
NOAA NMFS AMAPPS		The Atlantic Marine Assessment Program for Protected Species monitors marine mammals, sea turtles and sea birds along the entire east coast of the US. The AMAPPS website is: https://www.fisheries.noaa.gov/resource/publication-database/atlantic-marine-assessment-program-protected-species
ADEON	2017 - present	ADEON has deployed hydrophones at several locations in the Northwest Atlantic. One of their hydrophones is not far from CSI's hydrophone. The ADEON website is: https://adeon.unh.edu/
National Park Service (NPS)	2015 - 2018	NPS publishes annual reports of marine mammal strandings on the Cape Hatteras National Seashore, available at: https://www.nps.gov/caha/learn/nature/annualreports.htm
Cape Hatteras: Where Currents Collide	2004 - 2005	NSF funded field program. See https://www.whoi.edu/science/PO/hatterasfronts/

Materials & Methods

Deployments

Overview

For this NCROEP project, CSI has deployed a mooring on the continental slope off Cape Hatteras at 35°6' N, 75°5' W, at a depth of 230 meters. The mooring was equipped with a hydrophone, a CTD, and an Acoustic Doppler Current Profiler (ADCP). The first deployment lasted from late January of 2015 to late August of 2015. After the first mooring was retrieved, a second one was deployed to the same location. The hydrophone on the second deployment recorded sound from early September 2015 to late April 2016. A third deployment in 2019 successfully recorded data at this location from June to November.

Approximately 13 km to the northeast of the NCROEP mooring at a depth of 294 meters, the Atlantic Deepwater Ecosystem Observatory Network (ADEON) has deployed a mooring since November 2017 equipped with hydrophones, a CTD, and other instruments.

The table below summarizes the hydrophone deployments covered in this report.

	CSI CF1E	***CSI E663***	***ADEON EN615***	***CSI MAGI***
Dates	1/2015- 8/2015	9/2015- 4/2016	11/2017 – 6/2018	6/2019 – 11/2019
Location	35°6' N, 75°5' W	35°6' N, 75°5' W	35°11.987' N, 75°01.225' W	35°6' N, 75°5' W
Sample rate (samples/sec)	32,768	32,768	375,000	64,000
Duty factor	Recording 5 minutes out of every half -hour	Recording 5 minutes out of every half -hour	On for 1 minute and then off for 20 minutes	Recording 5 minutes out of every half -hour
Depth (meters)	230	230	294	230

CSI deployments (2015 – 2016)

For the first two CSI deployments, the mooring was equipped with a Multi Electronique Aural M2 hydrophone, a Seabird 37 SMP CTD, and a 150 kHz ADCP.

For these CSI deployments, the hydrophone was configured to sample at 32,768 samples per second. With this sample rate, the instrument's frequency range is from 10 Hz to 16,348 Hz. The hydrophone was configured to record for 5 minutes out of every half-hour.

CSI deployment (2019)

For this CSI deployment, the Aural M2 was upgraded with an M3 board, running in M3 mode. The sample rate was set to 64k samples/second. As in the previous CSI deployment, the hydrophone was configured to record for 5 minutes out of every half-hour.

ADEON deployment (2017 – 2018)

I obtained ADEON high-frequency hydrophone data at the Cape Hatteras site (HAT) for the EN615 deployment from the Passive Acoustic Data Archive at the NOAA National Centers for Environmental Information (NCEI). Specifically, NCEI uncompressed the ADEON EN615 HAT dataset (adeon_en615 hat.amar509.9 data files) and delivered it to me as a set of wav files on a hard disk that I provided.

I obtained the CTD data for the ADEON EN615 HAT deployment from the ADEON data portal (https://adeon.unh.edu/data_portal).

For details on the ADEON instruments, see the ADEON hardware specification document (Martin et al., 2018) at the ADEON project standards web site (https://adeon.unh.edu/standards) as well as the EN615 cruise report at the ADEON data portal. These ADEON documents show that the ADEON Hatteras mooring was deployed at 35°11.987' N, 75°01.225' W at a depth of 294 meters. This deployment was from late November 2017 to mid-June 2018. On this mooring, the instruments of interest to us include the following: a JASCO Autonomous Multichannel Acoustic Recorder (AMAR) hydrophone and a Sea-Bird MicroCAT SBE-37 CT-DO logger to measure conductivity, temperature, and dissolved oxygen. The AMAR was configured to sample at 375,000 samples/second, cycling on for 1 minute and then off for 20 minutes.

Hydrophone data processing

Filtering and down-sampling for high-frequency analysis

Detections of clicks, whistles and quacks are here categorized as "high-frequency data analysis".

Before high-frequency data analysis of the ADEON wav files, I down-sampled by a factor of 4 to 93,750 samples/second after applying an anti-aliasing filter with a cut-off frequency of 32 kHz. The anti-aliasing filter was implemented using a 4th order Butterworth filter, applied forward and reverse, using matlab version 9.7.0.1319299 (R2019b) Update 5.

The CSI hydrophone data was neither filtered nor resampled prior to high-frequency data analysis.

The table below summarizes the filtering and sample rate used per deployment for the high-frequency analysis.

Deployment	***Original sample rate (per second)***	***Low-pass filtering (of original) prior to HF analysis (Hz)***	***Sample rate for HF analysis (per second)***	***Effective bandwidth for HF analysis (Hz)***
CSI (CF1E)	32,768	--	32,768	16,384
CSI (E663)	32,768	--	32,768	16,384
ADEON (EN615)	375,000	32,000	93,750	32,000
CSI (MAGI)	64,000	--	64,000	32,000

The ADEON hydrophone was filtered to have the same effective bandwidth as the CSI MAGI hydrophone, making it easier to compare these data.

Filtering and down-sampling for low-frequency analysis

Detections of fin whale 20 Hz calls and other baleen whale calls are here categorized as "low-frequency data analysis".

The table below summarizes the filtering and sample rate used per deployment for the low-frequency analysis.

Deployment	***Low-pass filtering (of HF) prior to LF analysis (Hz)***	***Sample rate for LF analysis (per second)***	***Effective bandwidth for LF analysis (Hz)***
CSI (CF1E)	1 kHz	2.048 kHz	1 kHz
CSI (E663)	1 kHz	2.048 kHz	1 kHz
ADEON (EN615)	1.875 kHz	9.375 kHz	1.875 kHz
CSI (MAGI)	1 kHz	4.096 kHz	1 kHz

Detecting clicks

With an effective bandwidth of only 16 kHz in CSI deployments CF1E and E663, the clicks that can be well sampled include sperm whale clicks (Goold and Jones, 1995) as well as the "megapclicks" of the humpback whale (Stimpert et al., 2007). The higher bandwidth of the later deployments (32 kHz), allows for detection of delphinids as well.

Clicks were detected using the built-in click detector of PAMGuard (version 2.01.05 beta), using default settings except for the following:

- detection threshold: 12 dB
- high-pass filter: 1 kHz

Some of the settings for PAMGuard's click detector were in units of *samples* instead of time. The default values were used for the lower-bandwidth deployments (CF1E and E663). For the higher-bandwidth deployments, these settings were adjusted accordingly, so that their values *in time* were consistent across all four deployments.

For each click detection, the following features were then extracted (using matlab) in order to classify the detections:

- peak frequency
- mean frequency
- bandwidth
- duration
- variance

Using these features, a Naïve Bayes classifier was trained to separate clicks from ship noise and other noise sources, reducing false alarms. Using Raven Lite, I then manually reviewed several recording intervals with a lot of clicks, making sure that false alarms were indeed removed.

Detecting whistles

For both CSI and ADEON hydrophone data, the Matlab-based tool Silbido (Roch et al., 2011) was used to automatically detect whistles in each of the recording intervals. Silbido was configured to look for whistles above 2 kHz. The SNR criterion was set to the default value of 10 dB. Before running Silbido on each recording interval, the recording was high-pass filtered with a cut-off frequency of 1 kHz. The "beta 2 (2015-03-11)" version of Silbido was used, from http://roch.sdsu.edu/Software.shtml. This version has a very low false alarm rate. Still, some post-processing was required in order to remove anthropogenic signals, including 12 kHz pings from side-scan sonar. This was accomplished programmatically.

After detecting individual whistles, I calculated the total duration of the detected whistles for each recording interval. I divided this value by the duration of the recording interval to obtain a normalized metric, the fraction of time spent whistling per recording interval. I shall refer to this metric as the "vocalization metric" (VM).

I did not attempt to classify the whistles by species. Previous studies (Oswald et al., 2004) suggest that one needs an effective bandwidth of at least 24 kHz to classify dolphin whistles by species. The effective bandwidth for the first two CSI deployments is only 16 kHz.

Detecting quacks

Dolphin quacks or barks are "burst-pulse" vocalizations (Luis, 2016). These sounds have pitch, like human vowels. Therefore, I tried to detect these signals using a pitch detector, swipep (Camacho and Harris, 2008). This pitch detector has an implementation in matlab at:

https://www.cise.ufl.edu/~acamacho/publications/swipep.m

Quack detection using swipep was performed on the first two CSI deployments (CF1E and E663), skipping any recording intervals with noise above a specified threshold. Recording intervals with one or more detections were reviewed manually to remove false alarms, using Raven Lite 2.0.1.

Detecting fin whale 20 Hz calls

For both CSI and ADEON hydrophone data, a custom detector was implemented in matlab, following the approach documented by Nieukirk et al. (2012). For each recording interval, I calculated the spectrum of the low-pass filtered recording interval. If the spectrum had a peak between 18 and 22 Hz, above a specified threshold, the recoding interval was flagged for fin whale 20 Hz pulses. Each of the flagged intervals was manually reviewed (using Raven Lite) to determine the presence of 20 Hz fin whale pulses, thus removing any false alarms.

Since the sampling rate of the low-pass filtered wav file is different for different deployments, I adjusted the analysis window accordingly, as follows:

Deployment	***Low-pass filtering (of HF) prior to LF analysis (Hz)***	***Sample rate for LF analysis (per second)***	***Analysis window (samples) for estimation of spectrum***
CSI (CF1E)	1 kHz	2.048 kHz	???
CSI (E663)	1 kHz	2.048 kHz	???
ADEON (EN615)	1.875 kHz	9.375 kHz	???
CSI (MAGI)	1 kHz	4.096 kHz	???

Detecting humpback whale calls

TBD

Detecting North Atlantic right whale calls

TBD

Detection summary

The following table summarizes the types of detections performed per deployment.

	CSI CF1E	***CSI E663***	***ADEON EN615***	***CSI MAGI***	***Tool(s)***
Clicks	✓	✓	✓	✓	PAMGuard + matlab-based supervised learning to reduce false alarms
Whistles	✓	✓	✓	✓	Silbido + matlab to remove 12 kHz echosounder pings
Quacks	✓	✓			Pitch detector (swipep) + manual review
Fin whale 20 Hz	✓	✓	✓	✓	Custom matlab + manual review
Humpback whale calls	TBD	TBD	TBD	TBD	TBD
North Atlantic right whale calls	TBD	TBD	TBD	TBD	TBD

Oceanographic data processing

Oceanographic data was processed for the first two CSI deployments (CF1E and E663) as well as ADEON EN615.

CSI ADCP

For the CSI ADCPs, current velocities were measured every ten minutes with 4m vertical resolution. Measurements were quality controlled based on IOOS 2015 specifications (IOOS, 2015). Currents were then hourly averaged, and concurrent mooring deployments were resampled into uniform time and depth grids.

CSI CTD

On the CSI mooring, temperature and salinity measurements were made every 10 minutes. Data were quality controlled based on IOOS 2016 specifications (IOOS, 2016). On the ADEON mooring, temperature and salinity measurements were made every 30 minutes.

For each deployment, bottom temperature was bandpass filtered from 6 cycles per year to 1 cycle per day. This filtering eliminated low frequency seasonal variability as well as high frequency tidal variability, leaving the fluctuations due to mesoscale variability, such as the meandering front of the Gulf Stream.

ADEON CTD

For details on the ADEON instruments, see the ADEON hardware specification document (Martin et al., 2018) at the ADEON project standards web site (https://adeon.unh.edu/standards) as well as the EN615 cruise report at the ADEON data portal.

SST data

For each mooring location (CSI and ADEON), I downloaded GHRSST Level 4 MUR Global Foundation Sea Surface Temperature Analysis (v4.1) data from ERDDAP at https://coastwatch.pfeg.noaa.gov/erddap/griddap/jplMURSST41, specifying a time interval spanning the deployment as well as a bounding box surrounding the two mooring sites. This yielded two csv files, one for CSI and one for ADEON, having SST as a function of latitude, longitude, and time. For this Level 4 SST product, the sample interval is one day, and the spatial resolution is 0.01 degrees latitude by 0.01 degrees longitude. To obtain a SST time series for each mooring, I chose the values at the closest grid point.

The SST time series for each mooring was high-pass filtered at 6 cycles per year. Since the sample interval is once per day for SST, I did not need to filter out tidal variability. The filtering was implemented using a 4th order Butterworth filter, applied forward and reverse, using matlab version 9.7.0.1319299 (R2019b) Update 5.

Acoustic propagation modeling

To analyze and understand hydrophone data, one must also have an understanding of the acoustic propagation in the region of study. Of course, propagation modeling is also necessary if one wants to predict the impact of noise from turbines upon the surrounding marine life.

To model the acoustic propagation in the region of study, one needs sound speed as a function of depth and range. Since sound speed is a function of temperature, salinity, and pressure, one needs hydrographic data. For hydrographic data, I obtained nearby glider transects from Dr. Robert Todd of the Woods Hole Oceanographic Institution. The table below documents the glider data used in our analysis.

Glider	***WHOI Spray glider 15A065 Section 9***	***WHOI Spray glider 15C066 Section 7***
Dates	27-Oct-2015 to 31-Oct-2015	21-Jan-2016 to 26-Jan-2016
Coordinates (start and end of track)	(33.4729, -76.9195) to (33.8278, -74.6554)	(34.2641, -76.0166) to (34.7032, -73.1702)

Using these hydrographic data, I used two propagation modeling tools--bellhop, a ray-tracing tool as well as a matlab-based version of RAM, a parabolic equation (PE) based tool.

Results

Instrument Noise

Two sources of instrument noise can be found in the wav files from the CSI deployments.

First, an ADCP was co-located in the same mooring. It pinged once every 12 seconds. Each ping is a pulse of a 150 kHz sine wave. Although the hydrophone has an anti-alias filter, one can expect aliasing of the ADCP ping in the hydrophone recording. This is because the ADCP is relatively loud and close to the hydrophone, and the hydrophone's anti-alias filter is not a "brick wall". The frequency of the ADCP signal is less than a decade from the anti-alias filter's cut-off frequency. For these reasons, what gets recorded by the hydrophone could be an aliased "artifact" of the ADCP ping.

Whereas the ADCP artifact was present in all CSI deployments, there was another source of instrument noise seen only in the second CSI deployment (E663). As seen in Figure 3, some E663 recording intervals had a 1-second burst of broadband instrument noise, possibly from one of the other co-located instruments storing data to a hard-drive. It was not present in every recording interval.

Figure 3 below shows a spectrogram from deployment E663 having both sources of instrument noise—an unknown source of broad-band instrument noise between two ADCP pings.

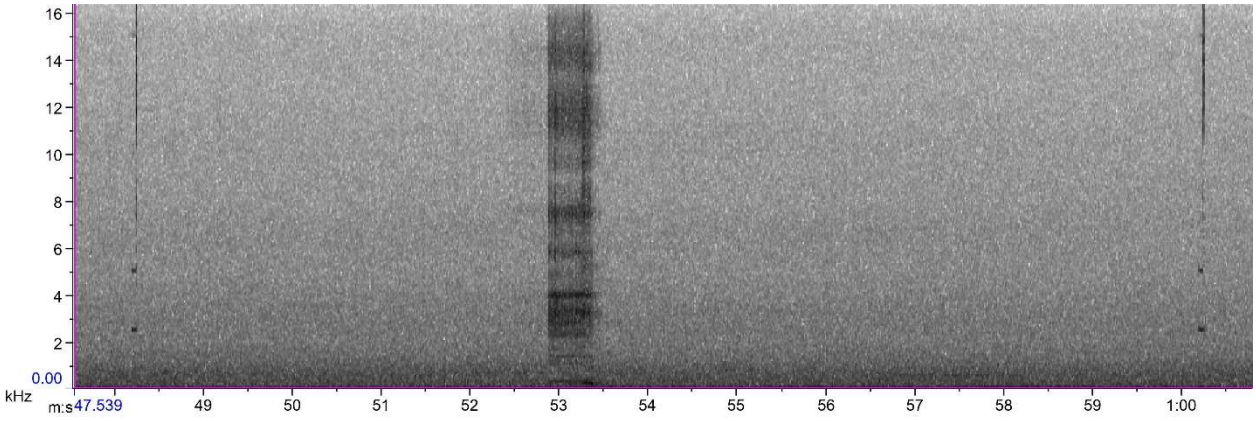

Figure 3: Two sources of instrument noise in CSI deployment E663. In this spectrogram, the x-axis is time in seconds, and the y-axis is frequency in kHz.

For the ADEON deployment, there was instrument noise from a co-located Acoustic Zooplankton Fish Profiler (AZFP), with pulses at four different frequencies--38 kHz, 125 kHz, 200 kHz, and 455 kHz.

Detections

Clicks

Given the 16 kHz bandwidth of CSI deployments CF1E and E663, the best species to target for click detection is the sperm whale (Goold and Jones, 1995) as well as the "megapclicks" of the humpback whale (Stimpert et al., 2007). For the higher frequency (32 kHz) deployments, I also looked for higher-frequency echolocation clicks from various odontocetes, including several species of dolphins and killer whales.

Reduce false alarms

Not all of PAMGuard's click detections were actually echolocation clicks. There were many false alarms due to instrument noise, ship noise, and environmental noise. To separate real echolocation clicks from noise, I used a machine learning approach similar to Zaugg et al. (2010). Using the following features (per PAMGuard click detection), a Naïve Bayes classifier was trained to separate clicks from noise, reducing false alarms:

- Peak frequency of the spectrum
- Mean frequency of the spectrum
- Bandwidth of the spectrum
- Duration
- Variance

For the deployments with *lower* bandwidth (16 kHz), the table below details the data that I used to train the classifier.

Classification	***Training data for CSI deployments CF1E and E663***
Signal	• Recording intervals from deployment CF1E with known clicks, with instrument noise removed • Examples of sperm whale clicks from the Watkins Marine Mammal Sound Database at Woods Hole Oceanographic Institution • Example of a humpback whale "megapclick"
Noise	• Known ship noise from deployment CF1E • Known environmental noise from deployment CF1E (i.e. intervals with high sea state), with instrument noise as well • Known instrument noise from both CF1E and E663

For the deployments with *higher* bandwidth (32 kHz), the table below details the data that I used to train the classifier, with differences underlined.

Classification	***Training data for deployments CSI MAGI and ADEON EN615***
Signal	• Recording intervals from these deployments with known clicks, with instrument noise removed • Examples of sperm whale clicks, dolphin clicks, and killer whale clicks from the Watkins Marine Mammal Sound Database at Woods Hole Oceanographic Institution • Example of a humpback whale "megapclick"
Noise	• Known ship noise from these deployments • Known environmental noise from these deployments (i.e. intervals with high sea state), with instrument noise as well, including known instrument noise from the ADEON AZFP

Figure 4 illustrates the classification of data from deployment CF1E, where the classifications are color-coded in a scatter plot of two of the five features. This figure shows that the variance is a key feature for separating actual clicks from noise.

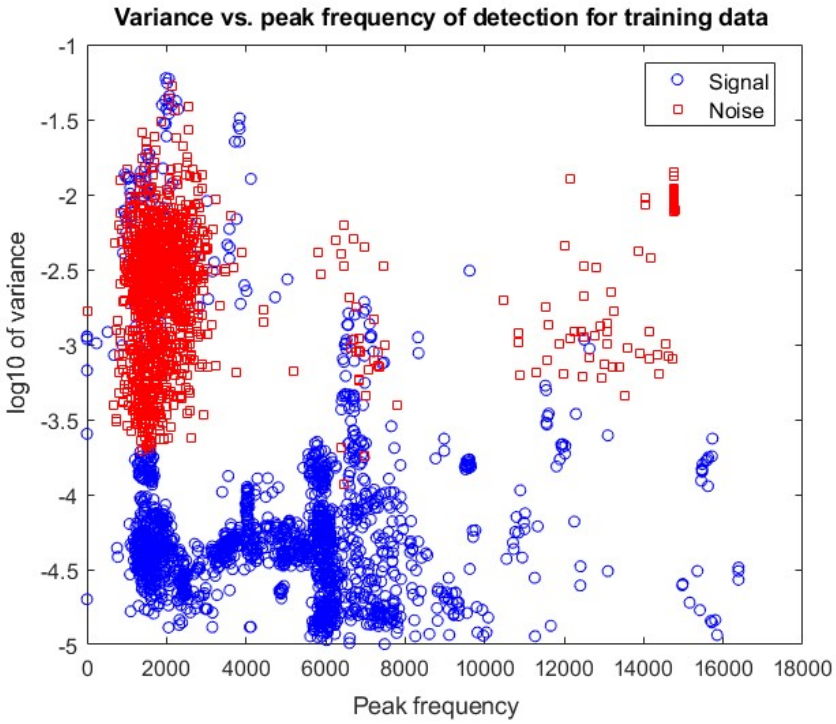

Figure 4: Example of classification using training data from deployment CF1E, showing a scatter plot for a pair of features. The training data was labeled as either Signal (in blue) or Noise (in red).

Temporal pattern

After reducing false alarms, I then calculated the average number of clicks per minute for each recording interval. Per deployment, Figure 5 shows a probability density function (PDF) of this metric.

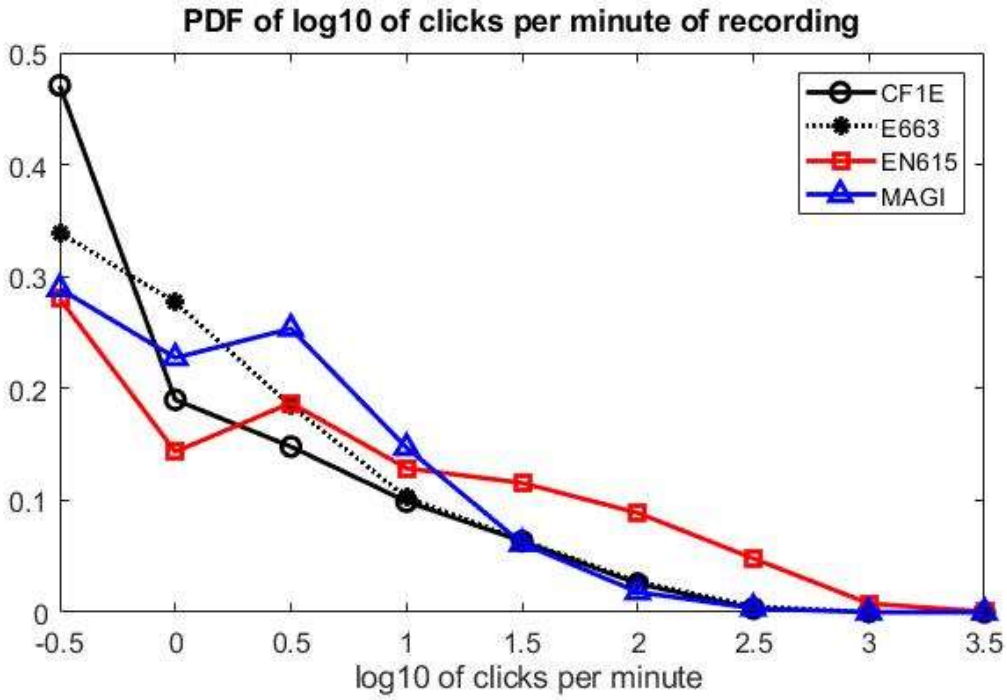

Figure 5: The distribution of the number of clicks per minute, for each deployment

Figure 6 below illustrates the temporal pattern of clicks per deployment by showing the fraction of recording intervals (per month) having more than a specified threshold of 10 clicks per minute.

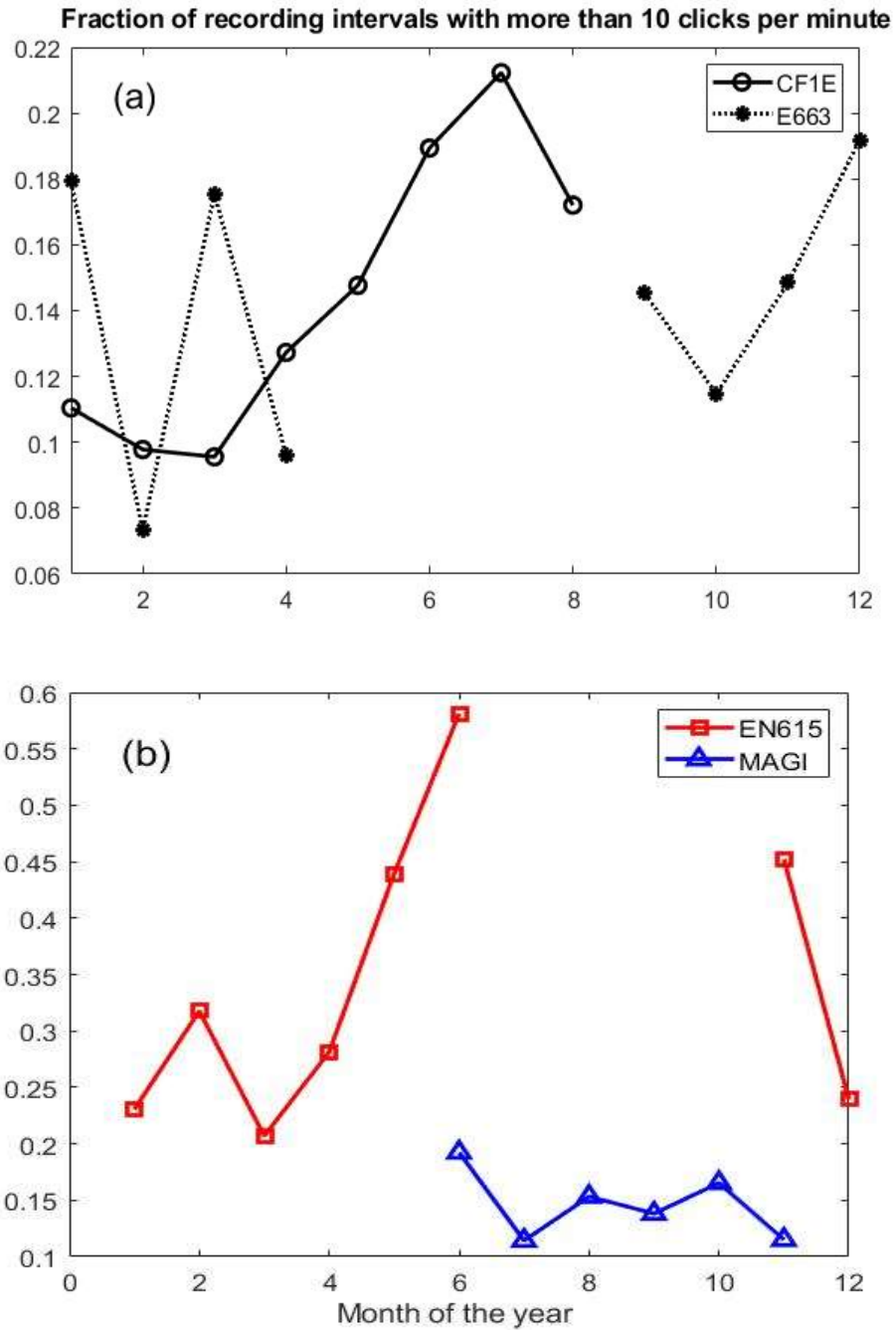

Figure 6: The fraction of recording intervals (per month) having more than 10 clicks per minute: a) for the first two CSI deployments (CF1E and E663) and b) for the later deployments, ADEON EN615 and CSI MAGI. Note that the scale for the y-axis changes from (a) to (b).

Figure 6 shows, for example, that if you listened at the ADEON site in June, the probability of hearing more than 10 clicks per minute would be almost 60%.

Figures 5 and 6 also show that the ADEON deployment had significantly more click detections than the CSI deployments. There are several possible explanations for the difference per deployment, including the following:

- Natural variability in space (the ADEON site is 13 km away from the NCROEP site) and time;
- The AMAR hydrophone used in ADEON EN615 has a greater sensitivity, compared to the AURAL M2 hydrophone used in the CSI deployments (as per correspondence with Bruce Martin of JASCO).
- The effective bandwidth is also increased for the later deployments (ADEON EN615 and CSI MAGI), 32kHz compared to 16,384 Hz for the first two CSI deployments.

Frequencies

For each click, I calculated the peak frequency of the spectrum. Figure 7 shows how this variable is distributed for each deployment. Note that the CF1E and E663 deployments are limited to a 16kHz bandwidth.

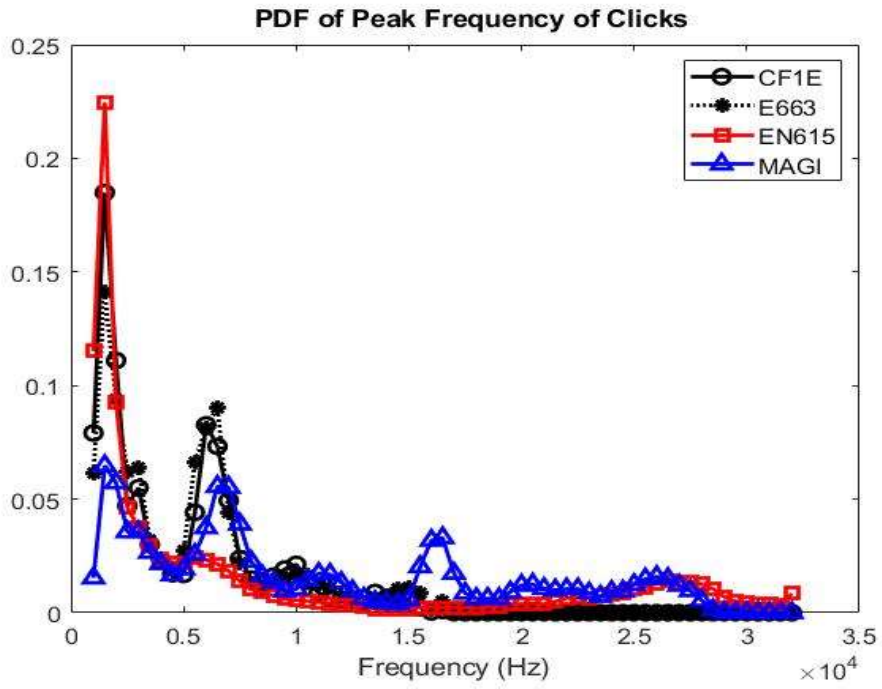

Figure 7: PDF of peak frequency of clicks, for each deployment

Figure 7 shows that the majority of the clicks have a peak frequency below 8 kHz. The PDF curves in Figure 7 have peaks at about 1.5 kHz and 6 kHz. This would be consistent with sperm whale clicks. The PDF for the MAGI deployment (in blue) also has a peak around 16 kHz.

Whistles

Temporal Pattern

For whistles, I calculated the fraction of whistling for each recording interval. A value of 1 would indicate that there was constant whistling during the entire recording interval. Per deployment, Figure 8 shows a probability density function (PDF) of this metric. Note that the y-axis is a log scale, and the bin centers (although consistent) are irregular.

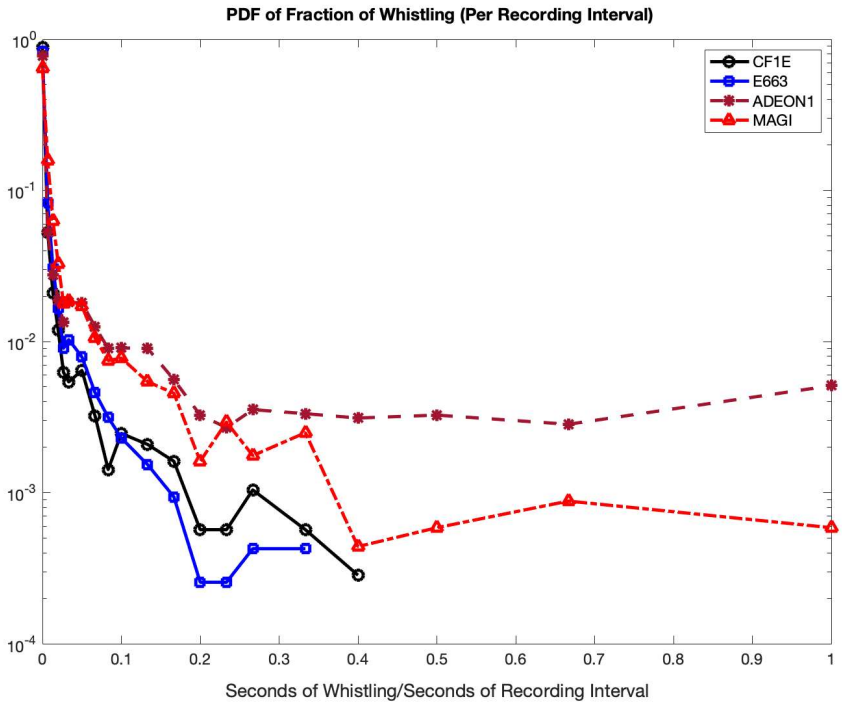

Figure 8: The distribution of the vocalization metric, fraction of time spent whistling (per recording interval) for each deployment

Figure 9 below illustrates the temporal pattern of whistles per deployment by showing the fraction of recording intervals (per month) having more than a specified threshold of 3 seconds of whistling per minute.

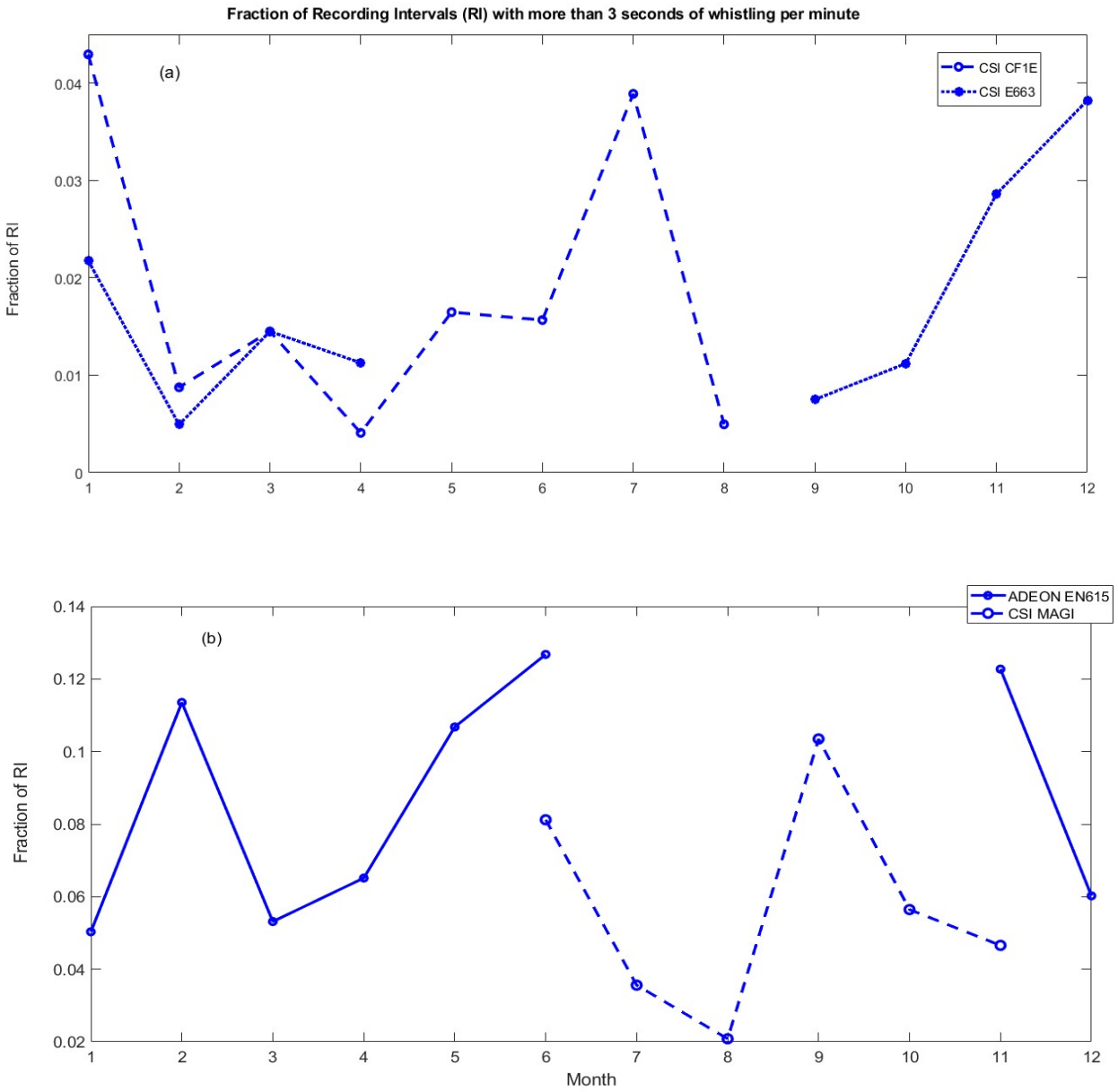

Figure 9: For each month of the year, the fraction of recording intervals with more than 3 seconds of whistling per minute of recording: a) for the first two CSI deployments (CF1E and E663) and b) for the later deployments, ADEON EN615 and CSI MAGI. Note that the scales are not the same in (a) and (b).

Figure 9 shows, for example, that if you listened at the NCROEP site in September, the probability of hearing more than 3 seconds of whistling per minute would be around 10% (according to MAGI), or less than 1% (according to E663).

Figures 8 and 9 plots show that the later deployments (ADEON EN615 and CSI MAGI) have several times the amount of whistling compared to the first two CSI deployments (CSI CF1E and CSI E663), and ADEON EN615 has more than CSI MAGI. As with the click detections, it is challenging to compare across deployments with different sites, sensors, and sample rates.

In Figure 8, data from ADEON EN615 and CSI MAGI indicate that there are some times when there is constant whistling for the entire recording interval. An example is shown below in Figure 10.

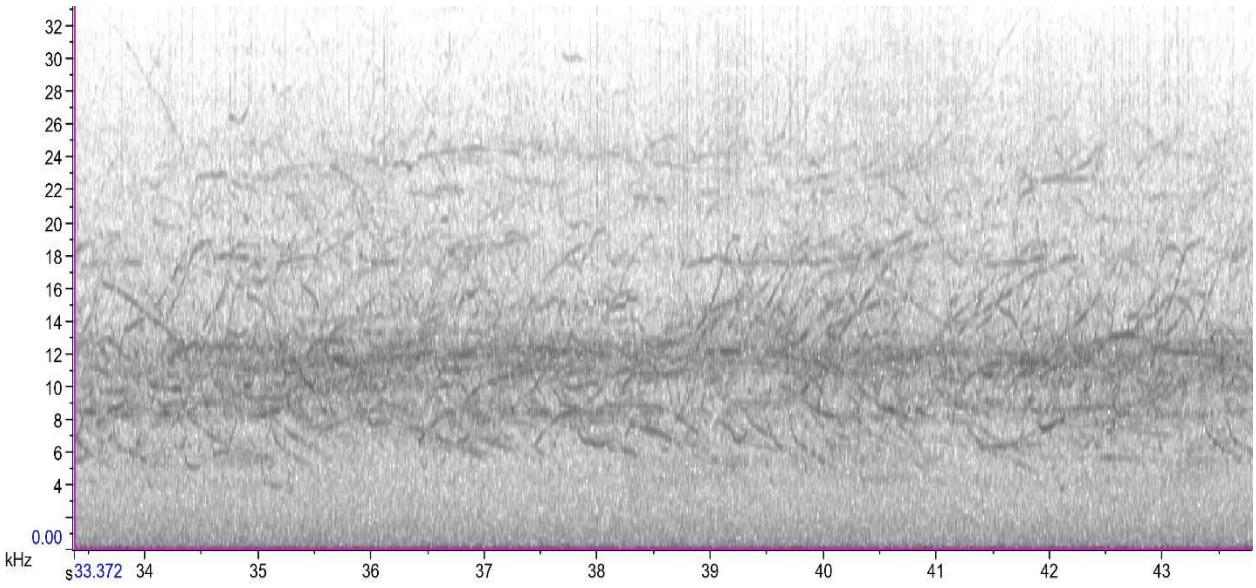

Figure 10: An example of constant, overlapping whistles, from ADEON file AMAR509.9.20180311T193056Z.wav. In this spectrogram, the x-axis is time in seconds, and the y-axis is frequency in kHz.

Frequencies

For each whistle, I calculated the median of the frequencies in the whistle. Figure 11 shows how this variable is distributed for each deployment. Note that the CF1E and E663 deployments are limited to a 16kHz bandwidth.

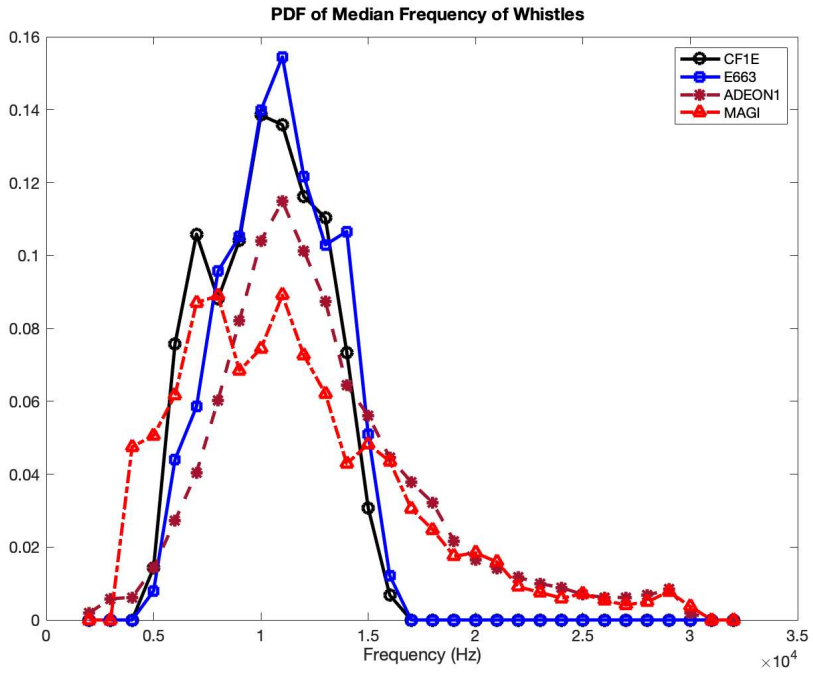

Figure 11: PDF of median frequency of whistles, for each deployment

For the CF1E, E663, and ADEON EN615 deployments, the most likely median frequency is around 10-11 kHz.

Quacks

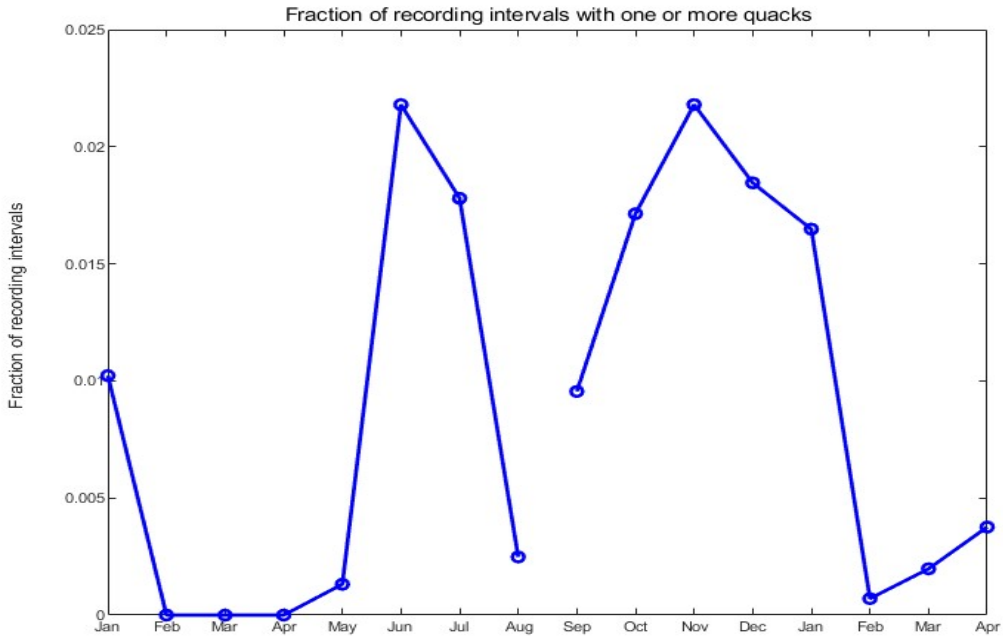

Figure 12: For the first two CSI deployments (CF1E and E663), the fraction of recording intervals (per month) with one or more quacks.

For the first two CSI deployments (CF1E and E663), Figure 12 shows the fraction of recording intervals (per month) with one or more dolphin quacks. The recording intervals with quacks are a subset of the recording intervals with whistles.

Fin whale 20Hz calls

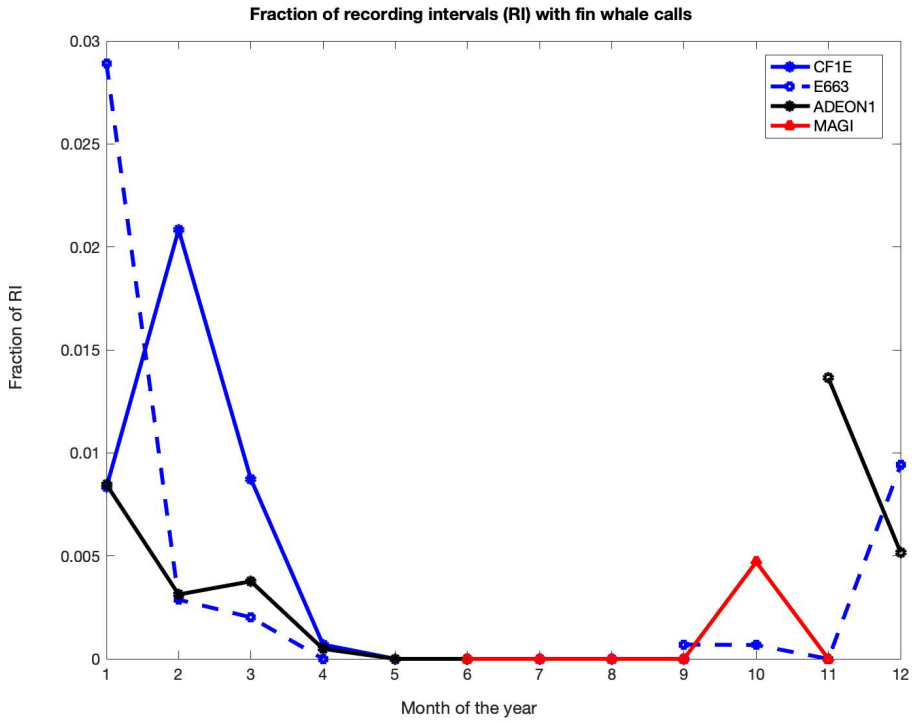

Figure 13: Temporal pattern of fin whale 20 Hz calls

Figure 13 shows the temporal pattern of fin whale 20Hz calls for each deployment. Deployments have peaks in November (ADEON EN615), January (CSI E663), and February (CSI CF1E). The MAGI deployment recorded only from late June to mid-November, likely missing the peak of the fin whale migration.

Humpback whale calls

TBD

Figure 14: Temporal pattern…

North Atlantic right whale calls

TBD

Figure 15: Temporal pattern …

Long-term average spectra

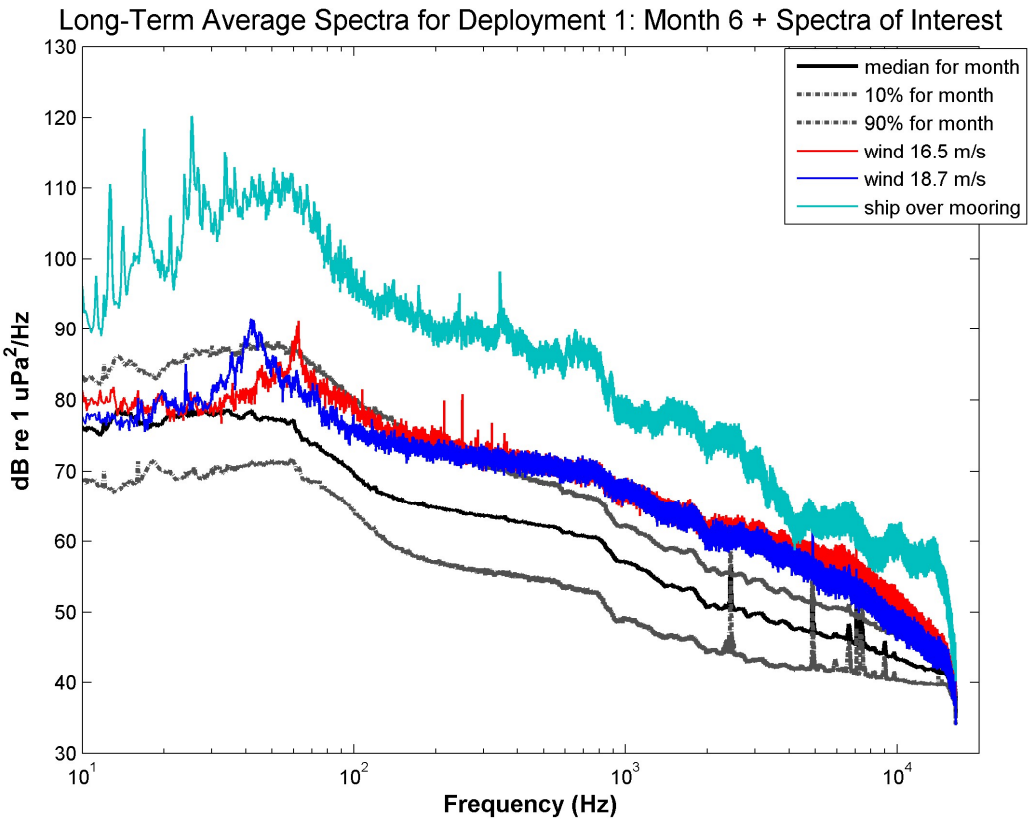

Figure 16: Long-Term Average Spectra (LTAS) were calculated for each 5-minute recording interval, using an analysis window of approximately 8 seconds. This figure shows statistics for an ensemble of LTAS for a representative month, July 2015. Statistics include the median (black), and 10- and 90-percentiles (gray). The figure also shows the LTAS for specific recording intervals when the winds were strong at the surface (red, blue) and when the CSI research vessel was underway directly over the mooring (turquoise).

Figure 16 shows long-term average spectra (LTAS) for the month of July 2015 as well as LTAS for several specific recording intervals of interest—all from deployment CF1E. Note that the values for the spectra rely on factory calibrations, not in situ calibration.

Correlation of marine mammal vocalizations to oceanographic features

Since previous studies have linked marine mammal abundance to enhanced productivity at frontal boundaries (Bost et al., 2009; Woodworth et al., 2012; Gilles et al., 2013), I looked for a relationship between marine mammal vocalizations and environmental variables. For CSI deployments CF1E, E663, and ADEON deployment EN615, I compared both bottom temperature and sea-surface temperature to the amount of whistling.

Bottom temperature

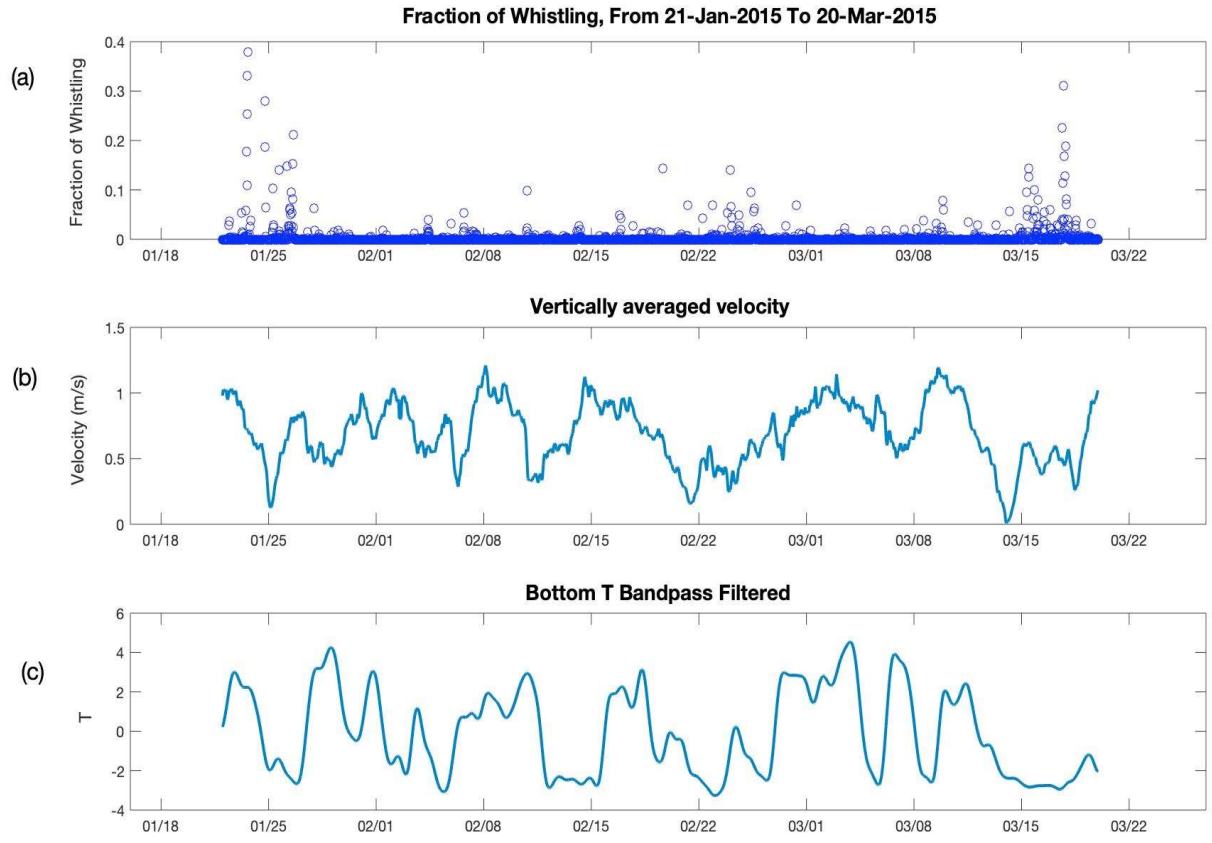

Figure 17: These three plots zoom in on the winter of 2015, during the first CSI deployment. In the top plot (a) is the marine mammal vocalization metric. In the middle plot (b), from the ADCP, the vertically averaged along-stream velocity. The bottom plot (c) shows the bandpass-filtered bottom temperature.

Figure 17 shows time series for the vocalization metric, bandpass-filtered bottom temperature (T_BP), and vertically-averaged water velocity for CSI in the winter of 2015. In this figure, if there is a lot of whistling (a), it seems likely that the velocity above the mooring (b) is low, and T_BP (c) is negative, indicating a cooler bottom temperature.

I then compared the vocalization metric (VM) to the bandpass filtered in situ bottom temperature (T_BP), looking for a relationship between VM and the environmental variable. This relationship will not necessarily be linear. For example, there may be a lot of vocalizations when the water is cooler, but the converse may not necessarily be true. In Woodworth et al. (2012), the authors segmented the physical data, sea surface height (SSH) based upon the biological data (presence/absence of melon headed whales). They then used the Kolmogorov-Smirnoff (KS) test to see if the two subsets of SSH were statistically different distributions.

I tried a similar approach. First, I interpolated the environmental variables T_BP to the time base of the VM. I then segmented T_BP into two subsets:

1) A "high vocalization" subset T_BP_{HV} consisting of the temperature samples that were acquired when VM was greater than a threshold and
2) A "low vocalization" subset T_BP_{LV} consisting of the temperature samples that were acquired when VM was less than or equal to the threshold.

For each deployment, the VM threshold was set to the 90th percentile value of the VM values for that deployment.

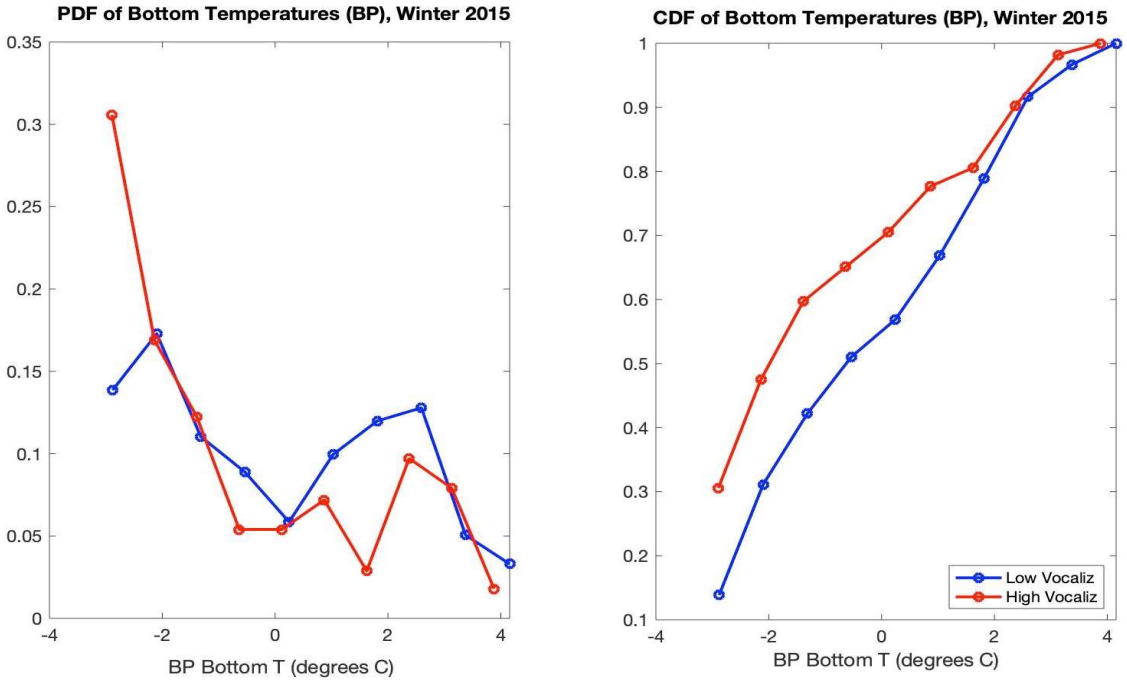

Figure 18: PDF and CDF of bottom temperature for the winter of 2015. The "high vocalization" subset is shown in red. The "low vocalization" subset is shown in blue.

For each season, I looked at the probability density function (PDF) and the related cumulative distribution function (CDF) of these subsets. For example, in Figure 18, I plot the PDF and CDF of both T_BP_{HV} (in red) and T_BP_{LV} (in blue) during the winter of 2015. In this figure, the distribution of the "high vocalization" subset is skewed to the colder water, relative to the distribution of the "low vocalization" subset.

Sea-surface temperature

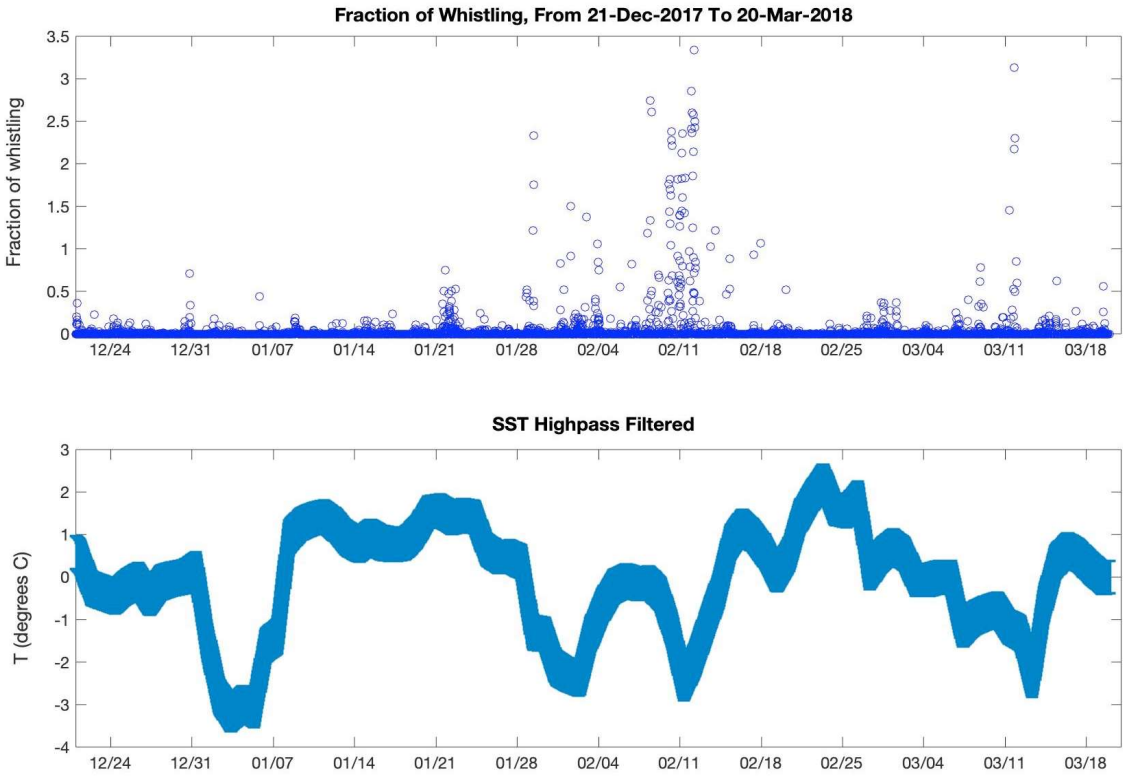

Figure 19: These two plots zoom in on the winter of 2018, during the ADEON EN615 deployment. The top plot shows the marine mammal vocalization metric. The bottom plot shows the high-pass filtered bottom temperature with error bars of +/- one standard deviation.

Figure 19 shows a time series for the vocalization metric as well as the high-pass filtered sea surface temperature for ADEON in the winter of 2018. The plots show that there are four events in the winter of 2018 when the highpass-filtered SST dropped below -2 degrees C. (This corresponds to SST below 20 degrees C for this period.) Analysis of SST images (not shown) reveals that—in all four cases—the mooring location was very close to the Gulf Stream front but on the denser, cooler side. For three out of the four events, vocalizations were very high, above the 90th percentile threshold for the ADEON deployment.

Like the band-pass filtered bottom temperature, the high-pass filtered SST was divided into two subsets, one corresponding to low values of the VM, the other corresponding to high values of the VM.

Wilcoxon rank sum test

After segmenting the environmental data, I had the following subsets:

Environmental variable	***High Vocalization Subset***	***Low Vocalization Subset***
Bandpass-filtered bottom temperature	T_BP_{HV}	T_BP_{LV}
Highpass-filtered SST	SST_HP_{HV}	SST_HP_{LV}

To quantify the difference between the two subsets, I then performed the Wilcoxon rank sum test (van Belle, 2004). In general, for each environmental variable X, I then used this statistical test to compare the high-vocalization subset X_{HV} to the low-vocalization subset X_{LV} to see if their medians were statistically different. Specifically, to quantify the difference between the two subsets (X_{HV} and X_{LV}), I created the following features:

- The difference between the median values: diff_Medians = median(X_{HV}) - median(X_{LV})
- The p-value from the rank sum test: p-value = ranksum(X_{HV},X_{LV})

where environmental variable X is either T_BP or SST_HP.

Our hypothesis is that the water is cooler when there are more vocalizations. This would be the case if the following were true:

- diff_Medians is negative (indicating cooler water in the high-vocalization set)
- abs(diff_Medians) is large, indicating the two subsets are different
- The p-value is less than 0.01, indicating that the two subsets are statistically different with 99% confidence.

The data analysis was accomplished using Matlab version 9.7.0.1319299 (R2019b) Update 5.

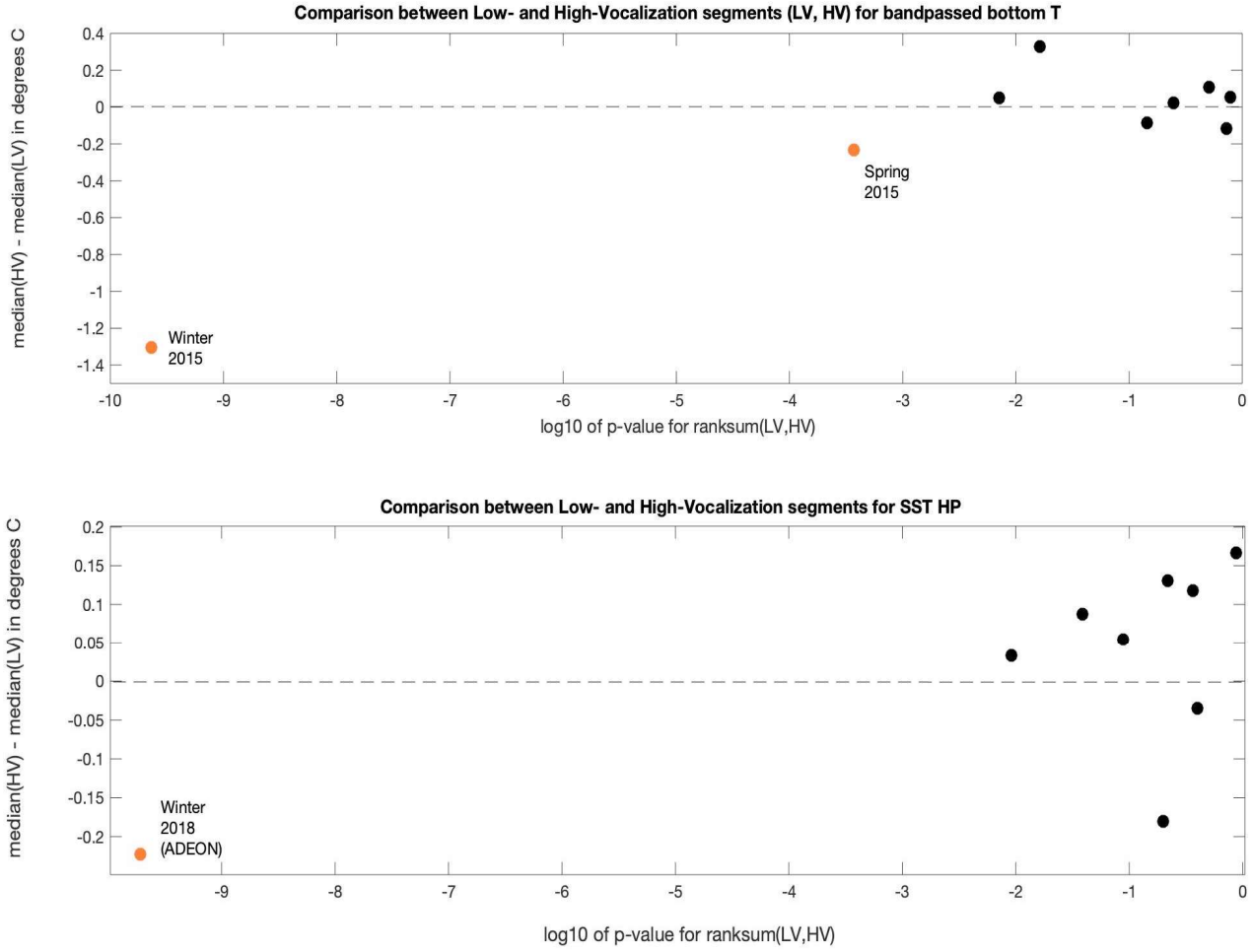

Figure 20: The results of the Wilcoxon rank sum test are presented here as scatter plots. Each point represents a season. On the x-axis is log10(p-value) from the rank-sum test. On the y-axis is diff_Medians. The plot on top is for bandpass-filtered bottom temperature, and the plot on the bottom is for highpass-filtered SST. If our hypothesis is confirmed for a season, it is color-coded orange; otherwise, it is color-coded black.

Figure 20 summarizes the results of this statistical test by plotting the two features (diff_Medians and p-value) in a scatter plot for each season. The top plot in this figure shows the results for bandpass-filtered bottom temperature. During the winter of 2015 and to a lesser extent the spring of that year (in orange), the bottom temperature for the high-vocalization subset was cooler and statistically different from that of the low vocalization subset. One could not say the same for the other seasons (in black), where either the p-value is too high or the difference between the medians is not negative.

Similarly, the bottom plot in Figure 20 summarizes the results from comparing the two subsets of high-pass filtered sea surface temperature SST_HP_{HV} and SST_HP_{LV}. This plot shows that during the winter

of 2018 (in orange), the SST for the high-vocalization subset was cooler and statistically different from that of the low vocalization subset. One could not say the same for the other seasons (in black), where either the p-value is too high or the difference between the medians is not negative

Water mass considerations

Can we be sure that the cooler water sampled at the mooring during the "high vocalization" periods is actually due to upwelling into the meander trough and not some other water mass? Could it be shelf water cascading down the slope?

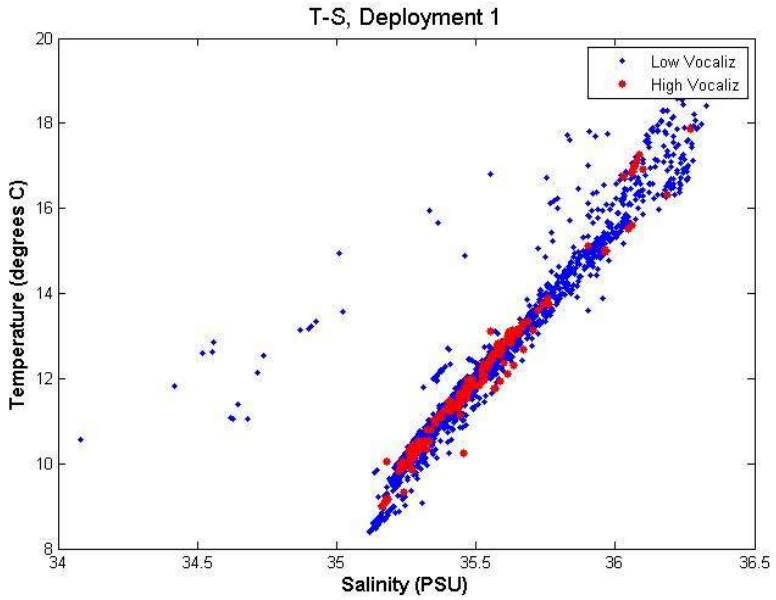

Figure 21: T-S plot for the first deployment. The "high vocalization" set is shown in red, and the "low vocalization" set in blue.

A water mass can be characterized by its temperature and salinity values. Figure 21 shows the T-S curve from the CTD data of the first deployment, a scatter plot of bottom temperature vs. bottom salinity for both the "low vocalization" set (in blue) and the "high vocalization" set (in red).

The Gulf Stream is a distinct water mass with a characteristic temperature-salinity (T-S) curve. If the temperature and salinity from the mooring's CTD data fall on this characteristic curve, we can be confident that we are measuring Gulf Stream water and not some other water mass.

To construct a representative T-S curve for the Gulf Stream in this region, we used a nearby glider transect, provided by Dr. Robert Todd of the Woods Hole Oceanographic Institution. This glider sampled the western half of the Gulf Stream just south of our mooring site in January of 2016. Figure 22(a) shows a transect of temperature from this glider.

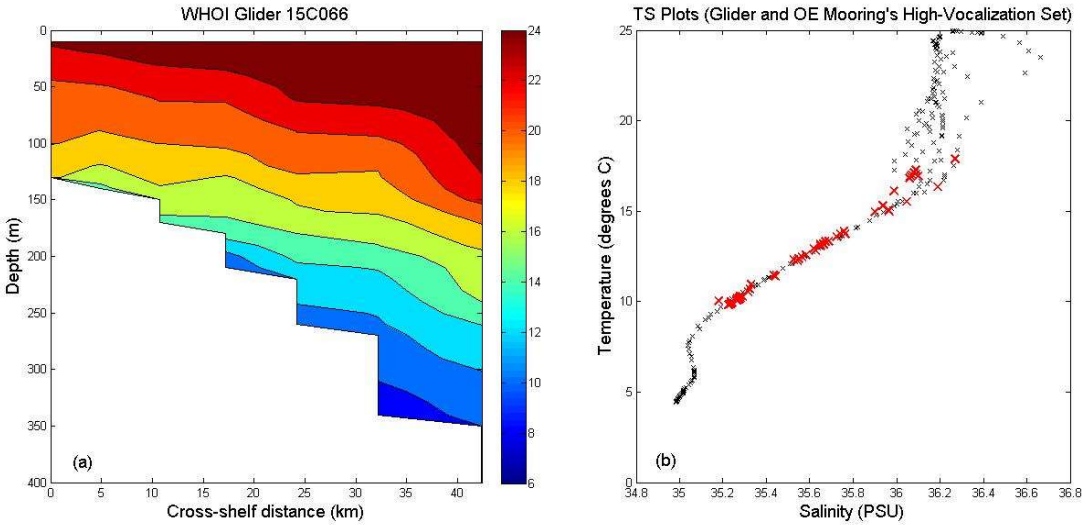

Figure 22: (a) Transect of temperature (in degrees C) across the western half of the Gulf Stream during January of 2016 based on WHOI Spray glider data. (b) T-S plot (in black) of the same glider transect as well as the T-S values from our mooring during "high vocalization" intervals (in red) in the winter of 2015.

Figure 22(b) shows the T-S plot for this glider transect (in black) as well as the T-S values from the mooring during "high-vocalization" intervals during the winter of 2015 (in red). The T-S values from the mooring and the glider coincide and also agree with historical Gulf Stream winter T-S values in the region (Pietrafesa et al, 1994); therefore, we conclude that this cooler, fresher water is indeed Gulf Stream water, upwelling into the meander trough—not shelf water cascading down the slope.

Note that our mooring's CTD did acquire a small number of samples that did *not* belong to the Gulf Stream. Looking at the scatter plot of T-S in Figure 21, one sees some lower-salinity points that stray from the main cluster. These data correspond to rare and brief events where shelf water *was* cascading down the continental slope, a process known as "slumping" (Shapiro et al., 2003).

Acoustic propagation

Acoustic propagation near the hydrophone

I used bellhop, a ray-tracing propagation modeling tool, to model the propagation in the region around the NCROEP mooring. Sound speed profiles were derived from temperature and salinity profiles from a nearby glider, WHOI Spray glider 15A065 Section 9. Figure 23 shows three possible fates for sound produced here at a depth of 50 meters:

a) Non-propagating, surface: rays (in red) that hit the surface but do not propagate farther
b) Non-propagating, bottom-to-surface: rays (in blue) that hit the bottom at too steep an angle
c) Propagating, bottom-trapped: rays (also in blue) that reflect from the bottom but do not make it to the surface, instead refracting back down to the bottom

In the region around the NCROEP mooring, the sound that propagates down the slope is “bottom trapped”.

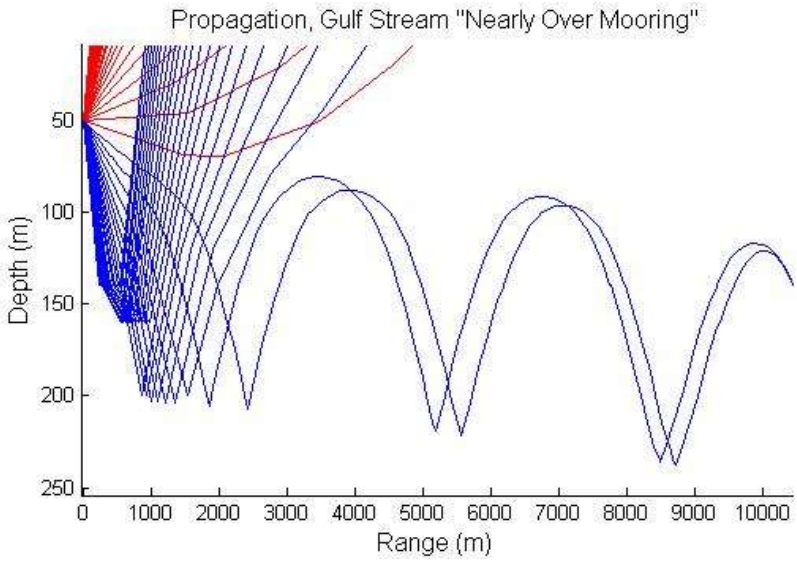

Figure 23: Output of bellhop for a sound source at 50 meters, using temperature and salinity profiles from a nearby glider, WHOI Spray glider 15A065 Section 9

Enhanced propagation in a Gulf Stream meander trough

Previous studies (Beckerle et al., 1980) have measured enhanced propagation through a cold-core ring. The cyclonic circulation in the cold-core ring induces upwelling, lifting the isotherms. As a result, the sound channel along the bottom becomes taller. This enhances the propagation because the sound can travel farther between expensive bottom bounces. These studies are relevant because a meander trough also has upwelling, induced by cyclonic circulation. Therefore, one may expect enhanced acoustic propagation in the region around the mooring when the mooring is in a meander trough—i.e. when the Gulf Stream moves far offshore.

Longer-range acoustic propagation model

Over longer distances, Carman and Robinson (1994) modeled the propagation of sound across the Gulf Stream, from the slope to the Sargasso Sea, at frequencies 25, 50, and 100 Hz. The authors discuss several factors that enhance the seaward propagation.

First, bottom loss is dependent upon the angle of incidence. In the seaward direction, the bottom is sloping down; therefore, the loss due to a bottom bounce is lower than it is in the shoreward direction. Second, the sound speed channel eventually detaches from the bottom. D'Amico (1980) shows this happening at a depth of 1200 meters. In this deep-sea sound channel, the propagation is ideal, as there are no interactions with the boundaries—neither surface nor bottom bounces. Therefore, if "bottom trapped" sound generated at the NCROEP site can make it to the deep-sea channel, it can propagate farther seaward for many tens of kilometers.

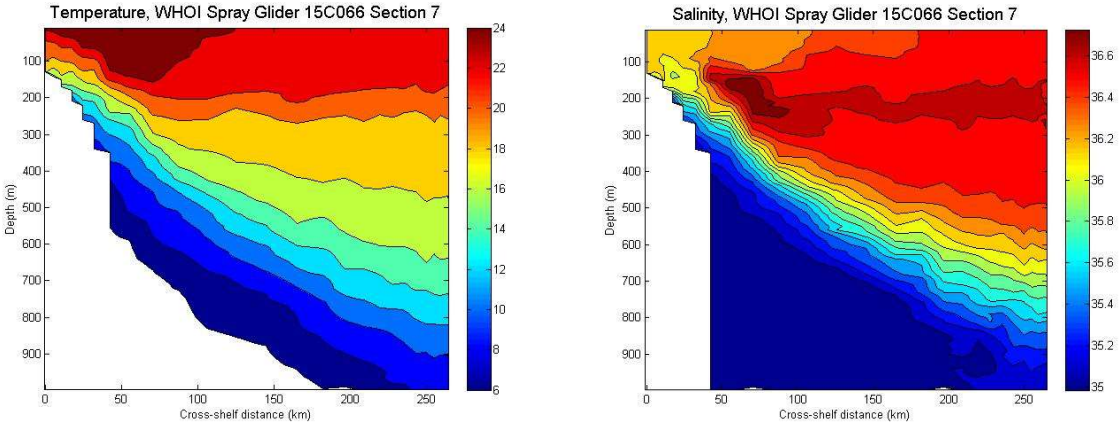

Figure 24: Cross-shelf temperature and salinity contours for WHOI Spray glider 15C066 Section 7

Using temperature and salinity from WHOI Spray glider 15C066 Section 7 (shown in Figure 24), I derived sound speed profiles. Using RAM, I then derived transmission loss as a function of range and depth (in Figure 25) with a sound source of 75 Hz at a depth of 200m (30m above our mooring).

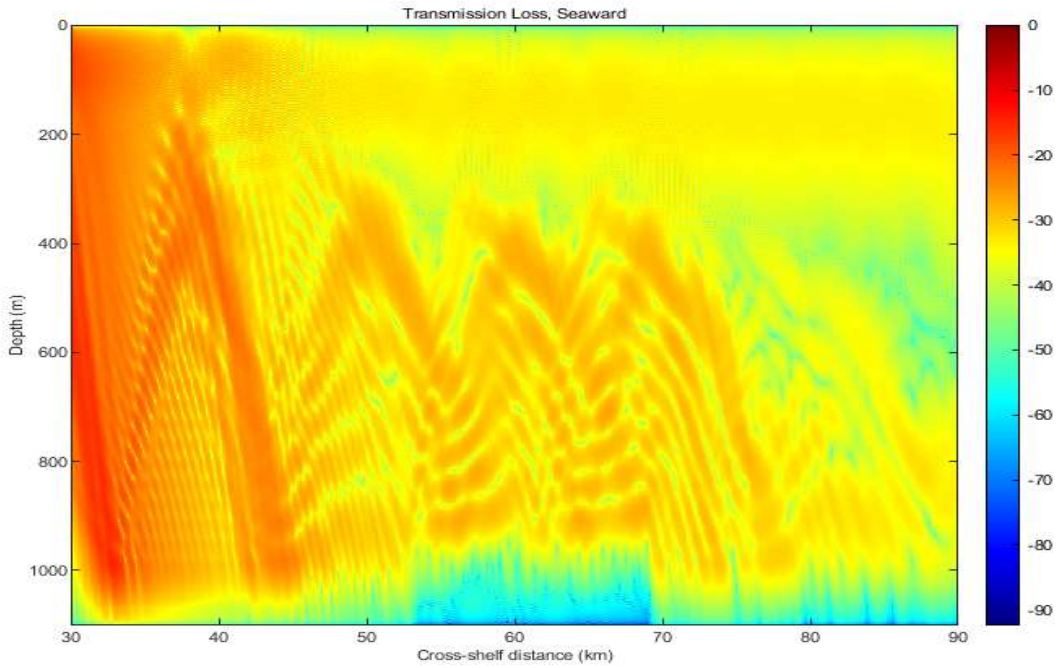

Figure 25: Acoustic propagation model, using RAM, given the temperature and salinity data from WHOI Spray glider 15C066 Section 7. The model shows transmission loss as a function of depth and range.

Quantitatively, the absolute values for transmission loss in Figure 25 are likely inaccurate, as I lack information about the bottom properties; however, the model is useful *qualitatively*. It shows not only a deep sound channel extending seaward but also a near-surface sound channel. D'Amico (1980) discussed a near-surface sound channel here due to "the entrainment of shelf water along the north edge of the Gulf Stream near Cape Hatteras".

Either the near-surface channel or the deep-sea channel would enhance the seaward propagation of low-frequency sound from the NCROEP site.

Conclusions

After analyzing the CSI and ADEON hydrophone data as well as the ancillary oceanographic data, I make the following conclusions:

Ship noise

Since the spectrum of a known source of loud ship noise was 10-20 dB higher than the 90th percentile (in Figure 16), one may conclude that loud ship noise was a relatively rare event in this region during the period of this study. Apparently, marine mammals in this region benefit from an environment that is relatively quiet.

Environmental noise

Environmental noise due to high sea states fell around the 90th percentile of the long-term average spectra (in Figure 16), a reasonable observation.

Acoustic propagation

Sound generated near the NCROEP mooring site would be bottom-trapped, propagating in a channel along the bottom. If it survived multiple bottom bounces, it could reach a deep sound channel, which detaches from the bottom at a depth of approximately 1200 meters. Once in this deep-sea channel, low-frequency noise could propagate tens of kilometers offshore.

In addition to a deep sound channel offshore, a near-surface sound channel may also form, possibly due to entrainment of fresher slope water near the surface. This finding is consistent with previous studies.

Detections

The literature provides ample evidence that this region is a “hot spot” for marine mammals. In general, the hydrophone data analysis is consistent with these previous studies. Below I summarize the findings for clicks, whistles, dolphin quacks, and several types of baleen whale vocalizations.

Clicks

Given the peak frequencies of the clicks detected by PAMGuard, these are likely sperm whales (Goold and Jones, 1995). It is challenging to see a consistent temporal pattern across all four deployments, but it is safe to say that clicks were detected in this region year-round.

Whistles

Similarly, whistles were detected year-round. Whistles were not classified by species, but previous studies suggest that the species detected could include several species of dolphins as well as short-finned pilot whales (Baird et al., 2015; Thorne at al., 2017).

Dolphin quacks

The recording intervals with dolphin quacks were shown to be a subset of the recording intervals with whistles. The temporal pattern has one peak in June and another peak in November.

Baleen whale vocalizations

As documented in Davis et al. (2020), many baleen whales pass through the waters around Cape Hatteras on their annual migrations. Regarding the temporal pattern of baleen whale calls off Cape Hatteras, the following table compares our findings to Davis et al. (2020).

Baleen whale species	*Our findings*	*Davis et al. (2020)*
Humpback whales	TBD	"Humpback whales were detected off Cape Hatteras… primarily between October and January, during their southward migration, with only a few detection days in spring and fall."
Fin whales	Peaks in November (ADEON EN615), January (CSI E663), and February (CSI CF1E).	Detected mostly at more northern latitudes. In the Cape Hatteras region, this species was detected mostly in fall and winter, with peak in January
North Atlantic right whales	TBD	Frequency of occurrence off Cape Hatteras was low, but increased in later years (2011-2014) compared to earlier years (2004-2010), possibly due to climate change.

Presumably, migrating baleen whales use the Gulf Stream to facilitate their poleward migration. On their way back equatorward, they need to stay shoreward of the fast-flowing Gulf Stream. On their *equatorward* journey, they are close enough to the hydrophones to be recorded.

Whistling at NCROEP site related to bottom temperature

When the Gulf Stream meanders farther offshore, cool, nutrient-rich water upwells in the region of the meander trough. This is the cool, nutrient-rich water that was measure at the NCROEP site when there was a lot of whistling during the winter and spring of 2015. Clearly, one would need more data to determine whether this is a trend. If and when we do get more data, we should also consider the following:

- Why would the observed relationship between whistling and bottom temperature be stronger in the winter? One possibility is that the species that we are observing migrates out of this region in the warmer months. In this region, a known population of bottle-nosed dolphins is usually found south of Cape Hatteras in the winter but north of the cape in the summer (Schick et al.,2011).

- It is possible that prey are attracted to the upwelling of cool, nutrient-rich water, leading to an actual increase in marine mammal abundance. Alternatively, the observed relationship between bottom temperature and vocalizations could be merely an acoustic propagation effect; in other words, the upwelling of cooler water may be improving the acoustic propagation in the region around the mooring.

- It is also possible that marine mammals are attracted to the Gulf Stream front regardless whether it is crest or trough. It may be that the NCROEP mooring is only close to the Gulf Stream front when the Gulf Stream meanders *off-shore* i.e. when the mooring is in the meander trough. Meander crests may be too far shoreward for the hydrophone to record activity at or near the front.

Whistling at ADEON site related to sea surface temperature

More data is obviously needed to see if there is a seasonal trend.

Acknowledgments

The Coastal Studies Institute project was funded by the North Carolina Renewable Ocean Energy Program. For ADEON data, I recognize the ADEON project sponsors (the US Department of the Interior, Bureau of Ocean Energy Management, Environmental Studies Program under contract # M16PC00003). I would like to thank the following colleagues:

- Dr. Michael Muglia of the Coastal Studies Institute and his team for preparing, deploying, and retrieving the moored instruments (hydrophone, ADCP, CTD).
- Sara Haines of the University of North Carolina at Chapel Hill for processing the CSI CTD and ADCP data.
- Dr. Robert Todd of WHOI for glider data.
- Veronica Martinez of NCEI in Boulder, Colorado for uncompressing the ADEON EN615 HAT dataset and delivering it to us as a set of wav files.
- Bruce Martin of JASCO Applied Sciences and ADEON Principal Investigator Dr. Jennifer Miksis-Olds of the University of New Hampshire for helpful discussions comparing the performance of the hydrophones.

References

Baird, R.W., Webster D.L., Swaim Z., Foley H.J., Anderson D.B., and Read A.J. 2015. Spatial use by Cuvier's beaked whales, short-finned pilot whales, common bottlenosed dolphins, and short-beaked common dolphins satellite tagged off Cape Hatteras, North Carolina, in 2014. Draft Report, Prepared for U.S. Fleet Forces Command. Submitted to Naval Facilities Engineering Command (NAVFAC) Atlantic, Norfolk, Virginia.

Beckerle J.C., Baxter L., Porter R.P., and R. C. Spindel. 1980. Sound channel propagation through eddies southeast of the Gulf Stream. The Journal of the Acoustical Society of America 68, 1750. doi: 10.1121/1.385220

Bost, C.A., Cotté C., Bailleul F., Cherel Y., Charrassin J.B., Guinet C., Ainley D.G., Weimerskirch H. 2009. The importance of oceanographic fronts to marine birds and mammals of the southern oceans. Journal of Marine Systems 78, 363–376.

Byrd B.L., Hohn A.A., Lovewell G.N., Altman K.M., Barco S.G., Friedlaender A.S., et al. 2014. Strandings as indicators of marine mammal biodiversity and human interactions off the coast of North Carolina. Fish Bull 112: 1–23. doi: 10.7755/FB.112.1.1.

Camacho A. and J.G. Harris. 2008. A sawtooth waveform inspired pitch estimator for speech and music. The Journal of the Acoustical Society of America 124, 1638. doi: 10.1121/1.2951592

Carman, J.C. and Robinson, A.R. 1994. Oceanographic, topographic, and sediment interactions in deep water acoustic propagation. Part II. Gulf Stream simulations. The Journal of the Acoustical Society of America 95, 1363. doi: 10.1121/1.408575

D'Amico A. 1980. Effects of the Gulf Stream on Acoustic Propagation SAIC Report SAI-81-221-WA

Davis G.E., Baumgartner M.F., Corkeron P.J., et al. 2020. Exploring movement patterns and changing distributions of baleen whales in the western North Atlantic using a decade of passive acoustic data. *Glob Change Biol*. 26: 4812– 4840. https://doi.org/10.1111/gcb.15191

Gilles A., Adler S., Kaschner K., Scheidat M., Siebert U. 2013. Modelling harbour porpoise seasonal density as a function of the German Bight. Endangered Species Research 22: 157-169.

Glenn S.M. and C.C. Ebbesmeyer, 1994. Observations of Gulf Stream frontal eddies in the vicinity of Cape Hatteras. J. Geophys. Res., 99(C3), 5047-5055.

Goold J.C. and Jones S.E. Time and frequency domain characteristics of sperm whale clicks. The Journal of the Acoustical Society of America, 1995, 98:1279-1291. doi:http://dx.doi.org/10.1121/1.413465

Hitchcock G.L., Mariano A.J., Rossby T. 1993. Mesoscale Pigment Fields in the Gulf Stream Observations in a Meander Crest and Trough. J. Geophys. Res., 98(C5), 8425-8445. doi:10.1029/92JC02911.

Hodge, L. Monitoring Marine Mammals in Onslow Bay, North Carolina, Using Passive Acoustics. PhD dissertation, Duke University, 2011, doi:http://hdl.handle.net/10161/4988

IOOS, 2015: Manual for real-time quality controls of in-situ current observations: A guide to quality control and quality assurance of acoustic Doppler current profiler observations. Version 2.0, accessed 23 Jun 2017, 51 pp. https://www.ioos.noaa.gov/wpcontent/uploads/2016/04/qartod_currents_manual.pdf

IOOS, 2016: Manual for real-time quality controls of In-situ Temperature and Salinity Data: A Guide to Quality Control and Quality Assurance for In-situ Temperature and Salinity Observations. Version 2.0, accessed 23 Jun 2017, 56 pp. [https://www.ioos.noaa.gov/wpcontent/uploads/2016/04/qartod_temperature_salinity_manual.pdf.]

Jahnke R.A. and Blanton J.O. 2010. The Gulf Stream. Chaper 3 in Carbon and Nutrient Fluxes in Continental Margins, Springer.

JPL MUR MEaSUREs Project. 2015. GHRSST Level 4 MUR Global Foundation Sea Surface Temperature Analysis (v4.1). Ver. 4.1. PO.DAAC, CA, USA.

Luís, A. R., Couchinho, M. N., & Dos Santos, M. E. (2016). A Quantitative Analysis of Pulsed Signals Emitted by Wild Bottlenose Dolphins. *PloS one*, *11*(7), e0157781. https://doi.org/10.1371/journal.pone.0157781

Martin B., Hillis C.A., Miksis-Olds J., Ainslie M.A., Warren J., and Heaney K.D. (2018). Hardware Specification. Document 01412, Version 2.3. Technical report by JASCO Applied Sciences for ADEON.

Martins A.M. and Pelegrí J.L. 2006. CZCS chlorophyll patterns in the South Atlantic Bight during low vertical stratification conditions. Continental Shelf Research. 26:429-457.

Nieukirk S.L., Mellinger D.K., Moore S.E., Klinck K., Dziak R.P., Goslin J. (2012) Sounds from airguns and fin whales recorded in the mid-Atlantic Ocean, 1999-2009. J Acoust Soc Am. 131(2):1102-12. doi: 10.1121/1.3672648. PMID: 22352485.

NOAA NMFS CRUISE RESULTS: NOAA Ship Gordon Gunter Cruise GU-06-03 (038), 19 June 19 -17 August, 2006

Olson, D., Hitchcock, G., Mariano, A., Ashjian, C., Peng, G., Nero, R., & Podestá, G. (1994). Life on the Edge: Marine Life and Fronts. *Oceanography, 7*(2), 52-60.

Osgood K.E., Bane J.M., and Dewar W.K. 1987. Vertical velocities and dynamical balances in Gulf Stream meanders. Journal of Geophysical Research, 92(c12),13029-13040,13211.

Oswald J.N., Rankin S., Barlow, J. (2004). The effect of recording and analysis bandwidth on acoustic identification of delphinid species. J. Acoust. Soc. Am. 116(5):3178–3185.

Pietrafesa L.J, Morrison J.M., McCann M.P., Churchill J., Bohm E., Houghton R.W. 1994. Water mass linkages between the Middle and South Atlantic Bights. Deep-Sea Research II, Vol. 41, No. 2/3, pp. 365 389.

Powell J. R., and Ohman M. D. (2015). Changes in zooplankton habitat, behavior, and acoustic scattering characteristics across glider-resolved fronts in the Southern California Current System. *Prog. Oceanogr.* 134, 77–92. doi: 10.1016/j.pocean.2014.12.011

Roch M.A., Brandes T.S., Patel B., Barkley Y., Baumann-Pickering, S., Soldevilla, M.S. (2011) Automated extraction of odontocete whistle contours. J. Acous. Soc. Am., 130(4), 2212-2223.

Savidge D. K. and Austin J. A. 2007. The Hatteras Front: August 2004 velocity and density structure. Journal of Geophysical Research: Oceans (1978–2012)112.C7.

Sayigh, L., Quick N., Hastie G., Tyack P. Repeated call types in short-finned pilot whales, Globicephala macrorhynchus. Marine Mammal Science, 2013, 29(2): 312-324. doi: 10.1111/j.1748-7692.2012.00577.x

Schick R.S., Halpin P.N., Read A.J., Urban D.L., Best B.D., Good C.P., Roberts J.J., LaBrecque E.A., Dunn C., Garrison L.P., Hyrenbach K.D., McLellan W.A., Pabst D.A., Palka D.L., Stevick, P. 2011. Community structure in pelagic marine mammals at large spatial scales. Mar. Ecol. Prog. Ser. 434: 165–181.

Shapiro G.I., Huthnance J.M., and Ivanov V.V. 2003. Dense water cascading off the continental shelf. J. Geophys. Res., 108(C12), 3390, doi:10.1029/2002JC001610

Stanistreet, J. E., D. P. Nowacek, J. T. Bell, D. M. Cholewiak, J. A. Hildebrand, L. E. W. Hodge, S. M. Van Parijs, & A. J. Read. Spatial and seasonal patterns in acoustic detections of sperm whales (Physeter macrocephalus) along the continental slope in the western North Atlantic. Endang Species Res 35: 1–13, 2018.

Stimpert, A. K., Wiley, D. N., Au, W. W., Johnson, M. P., & Arsenault, R. (2007). 'Megapclicks': acoustic click trains and buzzes produced during night-time foraging of humpback whales (Megaptera novaeangliae). *Biology letters*, *3*(5), 467–470. https://doi.org/10.1098/rsbl.2007.0281

Thorne L.H., Foley H.J., Baird R.W., Webster D.L., Swaim Z.T., Read A.J. (2017) Movement and foraging behavior of short-finned pilot whales in the Mid-Atlantic Bight: importance of bathymetric features and implications for management. Mar Ecol Prog Ser 584:245-257. https://doi.org/10.3354/meps12371

van Belle G., Fisher L.D., Heagerty P.J., Lumley, T. Biostatistics: A Methodology for the Health Sciences, 2nd Edition. 2004. John Wiley & Sons, Inc.

Woodworth, P.A., Schorr G.S., Baird R.W., Webster D.L., McSweeney D.L., Hanson M.B., Andrews R.D., and Polovina J.J. 2012. Eddies as offshore foraging grounds for melon-headed whales (*Peponocephala electra*). Marine Mammal Science 28: 638-647.

Zaugg S, M van der Schaar, L Houégnigan, C Gervaise, M André. Real-time acoustic classification of sperm whale clicks and shipping impulses from deep-sea observatories. *Applied Acoustics*, 2010, 71(11):1011-1019. http://dx.doi.org/10.1016/j.apacoust.2010.05.005.